Defense Threat Reduction Agency
8725 John J. Kingman Road, MS 6201
Fort Belvoir, VA 22060-6201

DTRA-TR-04-4

TECHNICAL REPORT

# *Low Noise Infrasonic Sensor System with High Reduction of Natural Background Noise*

Approved for public release; distribution is unlimited.

May 2006

DTRA 01-01-C-0050

F. Kern, et al.

Prepared by:
Physical Sciences Inc.
20 New England Business Center
Andover, MA 01810

## DESTRUCTION NOTICE

**FOR CLASSIFIED** documents, follow the procedures in DoD 5550.22-M, National Industrial Security Program Operating Manual, Chapter 5, Section 7 (NISPOM) or DoD 5200.1-R, Information Security Program Regulation, Chapter 1X.

**FOR UNCLASSIFIED** limited documents, destroyed by any method that will prevent disclosure of contents or reconstruction of the document.

Retention of this document by DoD contractors is authorized in accordance with DoD 5220.22M, Industrial Security manual.

PLEASE NOTIFY THE DEFENSE THREAT REDUCTION AGENCY, ATTN: IMMI, 8725 JOHN J. KINGMAN ROAD, MS-6201, FT. BELVOIR, VA 22060-6201. IF YOUR ADDRESS IS INCORRECT, IF YOU WISH IT DELETED FROM THE DISTRIBUTION LIST, OR IF THE ADDRESSEE IS NO LONGER EMPLOYED BY YOUR ORGANIZATION.

# DISTRIBUTION LIST UPDATE

This mailer is provided to enable DTRA to maintain current distribution lists for reports. (We would appreciate you providing the requested information.)

- ☐ Add the individual listed to your distribution list.
- ☐ Delete the cited organization/individual.
- ☐ Change of address.

Note:
Please return the mailing label from the document so that any additions, changes, corrections or deletions can be made easily. For distribution cancellation or more information call DTRA/BDMI (703) 767-4724.

NAME: _____

ORGANIZATION: _____

| OLD ADDRESS | NEW ADDRESS |
|---|---|
| _____ | _____ |
| _____ | _____ |
| _____ | _____ |

TELEPHONE NUMBER: (  ) _____

| DTRA PUBLICATION NUMBER/TITLE | CHANGES/DELETIONS/ADDITONS, etc. *(Attach Sheet if more Space is Required)* |
|---|---|
| _____ | _____ |
| _____ | _____ |
| _____ | _____ |

DTRA or other GOVERNMENT CONTRACT NUMBER: _____

CERTIFICATION of NEED-TO-KNOW BY GOVERNMENT SPONSOR (if other than DTRA):

SPONSORING ORGANIZATION: _____

CONTRACTING OFFICER or REPRESENTATIVE: _____

SIGNATURE: _____

DEFENSE THREAT REDUCTION AGENCY
ATTN: BDLMI
8725 John J Kingman Road, MS 6201
Fort Belvoir, VA 22060-6201

DEFENSE THREAT REDUCTION AGENCY
ATTN: BDLMI
8725 John J Kingman Road, MS 6201
Fort Belvoir, VA 22060-6201

| REPORT DOCUMENTATION PAGE | Form Approved OMB No. 0704-0188 |
|---|---|



| 1. AGENCY USE ONLY (Leave blank) | 2. REPORT DATE | 3. REPORT TYPE AND DATES COVERED |
|---|---|---|
| | May 2006 | Final Report, covering the period 26 September 2002 through 31 December 2003 |

**4. TITLE AND SUBTITLE**

Low Noise Infrasonic Sensor System with High Reduction of Natural Background Noise

**5. FUNDING NUMBERS**

C – DTRA 01-01-C-0050
PE – 13ND
PR – ND
TA – XX
WU – DH01135

**6. AUTHOR(S)**

F. Kern, S. Africk, P. Cataldi, R. Chaves

**7. PERFORMING ORGANIZATION NAME(S) AND ADDRESS(ES)**

Physical Sciences Inc.
20 New England Business Center
Andover, MA 01810

**8. PERFORMING ORGANIZATION REPORT NUMBER**

PSI-1370/TR-1896

**9. SPONSORING/MONITORING AGENCY NAME(S) AND ADDRESS(ES)**

Defense Threat Reduction Agency
8725 John J. Kingman Road, STOP-6201
Fort Belvoir, VA 22060-6201
NTD/D. Barber

**10. SPONSORING/MONITORING AGENCY REPORT NUMBER**

DTRA-TR-04-4

**11. SUPPLEMENTARY NOTES**

This work was sponsored by the Defense Threat Reduction Agency RTD&E RMSS Codes B 13ND D E310 ND XX 01135 25904D.

**12a. DISTRIBUTION AVAILABILITY STATEMENT**

Approved for public release; distribution is unlimited.

**12b. DISTRIBUTION CODE**

**13. ABSTRACT (Maximum 200 words)**

Physical Sciences Inc. has developed a new type of infrasound piezocable sensor system under this program's SBIR Phase I and Phase II funding from DTRA. The sensors consist of continuous lengths of off-the-shelf radially poled polyvinylidene fluoride (PVDF) coaxial cables, theoretically of arbitrary length, specially terminated and connected to state of the art, ultra high input impedance quiet amplifiers, tailored to the unique characteristics of the sensor outputs. Test data reported herein has primarily been collected with sensors of 100 m lengths deployed in the field after significant development, laboratory testing and system calibration efforts were undertaken. Pairs of such long line sensors deployed at right angles to each other can determine signal incidence direction and also eliminate the aliasing associated with the current infrasound sensors used at large spacing in the present designs of infrasound monitoring arrays, particularly in the higher frequency ranges of interest around 1 Hz. Prototype sensors have been utilized to collect data at Pinon Flat, CA (Infrasound Station-I57US) with support from Scripps, UCSD, and a sensor array is also installed in Hawaii at I59US with support from ISLA, University of Hawaii. This report presents some of the key results of field test measurements to document the capability of these new, robust, and inexpensive sensors.

**14. SUBJECT TERMS**

infrasonic pressure sensors, infrasonic vibration/earthquake sensors, PVDF piezo polymer sensors, ultraquiet high input impedance low frequency amplifiers

**15. NUMBER OF PAGES**

49

**16. PRICE CODE**

| 17. SECURITY CLASSIFICATION OF REPORT | 18. SECURITY CLASSIFICATION OF THIS PAGE | 19. SECURITY CLASSIFICATION OF ABSTRACT | 20. LIMITATION OF ABSTRACT |
|---|---|---|---|
| Unclassified | Unclassified | Unclassified | SAR |

Standard Form 298 (Rev. 8-98) (EG)
Prescribed by ANSI Std. Z39-18

## CONVERSION TABLE

Conversion Factors for U.S. Customary to metric (SI) units of measurement.

| MULTIPLY → / TO GET ← | BY → / BY ← | TO GET → / DIVIDE ← |
|---|---|---|
| angstrom | 1.000 000 x E -10 | meters (m) |
| atmosphere (normal) | 1.013 25 x E +2 | kilo pascal (kPa) |
| bar | 1.000 000 x E +2 | kilo pascal (kPa) |
| barn | 1.000 000 x E -28 | meter$^2$ ($m^2$) |
| British thermal unit (thermochemical) | 1.054 350 x E +3 | joule (J) |
| calorie (thermochemical) | 4.184 000 | joule (J) |
| cal (thermochemical/$cm^2$) | 4.184 000 x E -2 | mega joule/$m^2$ ($MJ/m^2$) |
| curie | 3.700 000 x E +1 | *giga bacquerel (GBq) |
| degree (angle) | 1.745 329 x E -2 | radian (rad) |
| degree Fahrenheit | $t_k = (t°f + 459.67)/1.8$ | degree kelvin (K) |
| electron volt | 1.602 19 x E -19 | joule (J) |
| erg | 1.000 000 x E -7 | joule (J) |
| erg/second | 1.000 000 x E -7 | watt (W) |
| foot | 3.048 000 x E -1 | meter (m) |
| foot-pound-force | 1.355 818 | joule (J) |
| gallon (U.S. liquid) | 3.785 412 x E -3 | meter$^3$ ($m^3$) |
| inch | 2.540 000 x E -2 | meter (m) |
| jerk | 1.000 000 x E +9 | joule (J) |
| joule/kilogram (J/kg) radiation dose absorbed | 1.000 000 | Gray (Gy) |
| kilotons | 4.183 | terajoules |
| kip (1000 lbf) | 4.448 222 x E +3 | newton (N) |
| kip/inch$^2$ (ksi) | 6.894 757 x E +3 | kilo pascal (kPa) |
| ktap | 1.000 000 x E +2 | newton-second/$m^2$ ($N-s/m^2$) |
| micron | 1.000 000 x E -6 | meter (m) |
| mil | 2.540 000 x E -5 | meter (m) |
| mile (international) | 1.609 344 x E +3 | meter (m) |
| ounce | 2.834 952 x E -2 | kilogram (kg) |
| pound-force (lbs avoirdupois) | 4.448 222 | newton (N) |
| pound-force inch | 1.129 848 x E -1 | newton-meter (N-m) |
| pound-force/inch | 1.751 268 x E +2 | newton/meter (N/m) |
| pound-force/foot$^2$ | 4.788 026 x E -2 | kilo pascal (kPa) |
| pound-force/inch$^2$ (psi) | 6.894 757 | kilo pascal (kPa) |
| pound-mass (lbm avoirdupois) | 4.535 924 x E -1 | kilogram (kg) |
| pound-mass-foot$^2$ (moment of inertia) | 4.214 011 x E -2 | kilogram-meter$^2$ ($kg-m^2$) |
| pound-mass/foot$^3$ | 1.601 846 x E +1 | kilogram-meter$^3$ ($kg/m^3$) |
| rad (radiation dose absorbed) | 1.000 000 x E -2 | **Gray (Gy) |
| roentgen | 2.579 760 x E -4 | coulomb/kilogram (C/kg) |
| shake | 1.000 000 x E -8 | second (s) |
| slug | 1.459 390 x E +1 | kilogram (kg) |
| torr (mm Hg, $0^0$ C) | 1.333 22 x E -1 | kilo pascal (kPa) |

*The bacquerel (Bq) is the SI unit of radioactivity; 1 Bq = 1 event/s.
**The Gray (GY) is the SI unit of absorbed radiation.

## Contents

## List of Figures

## List of Figures (Continued)

## List of Figures (Continued)

**Acknowledgments**

Physical Sciences Inc. wishes to express its appreciation to DTRA for funding this unique sensor development program and for the encouragement provided by Anton Dainty, the government's technical representative. We would also like to thank Dr. Michael Hedlin and Clint Coon of UCSD-Scripps who supported our data acquisition and deployment of sensor systems at Pinon Flat, and for allowing us to place sensors near others begin evaluated at that facility. We were fortunate to be supported by Laura Rogers, Claus Hetzer and Dr. Milton Garces of ISLA, U. Hawaii for supporting our installation of sensors near 159 US and supplying us with data recorded at that site.

**Summary**

Physical Sciences Inc. (PSI) has developed a new type of infrasound piezocable sensor system under this program's SBIR Phase I and Phase II funding from DTRA. The sensors consist of continuous lengths of off-the-shelf, radially poled polyvinylidene fluoride (PVDF) coaxial cables, theoretically of arbitrary length, specially terminated and connected to state of the art, ultra high input impedance quiet amplifiers, tailored to the unique characteristics of the sensor outputs. Test data reported herein has primarily been collected with sensors of 100 m lengths deployed in the field after significant development, laboratory testing and system calibration efforts were undertaken. Pairs of such long line sensors deployed at right angles to each other can determine signal incidence direction and also eliminate the aliasing associated with the current infrasound sensors used at large spacing in the present designs of infrasound monitoring arrays, particularly in the higher frequency ranges of interest around 1 Hz. Prototype sensors have been utilized to collect data at Pinon Flat, CA (Infrasound Station-I57US) with support from Scripps, UCSD, and a sensor array is also installed in Hawaii at I59US with support from ISLA, University of Hawaii. This report presents some of the key results of field test measurements to document the capability of these new, robust and relatively inexpensive, (~$ 1,000 per cable) sensors.

# 1. Introduction

## 1.1 Background

Physical Sciences Inc. (PSI) completed its work on this DTRA-sponsored SBIR Program entitled "Low Noise Infrasonic Sensor System with High Reduction of Background Noise." During this program we developed a new and innovative infrasound sensor based on piezoelectric cable. Currently eight prototype sensor cables are installed in arrays at Pinon Flat, CA and a second array consisting of three cables is installed in Kona Hawaii. Furthermore, we have sufficient parts to assemble and install a third array at another site. Based on our SBIR work we believe that the technology is now ready for continuing data collection and analysis. Consequently we are proposing to operate a data collection network with these three sensor arrays to explore various operational configurations and data processing options. These data will be exploited to design optimized robust and easily portable sensor arrays. Multiple sensors will then be fabricated and deployed in support of Government specified experiments. The collected data will be analyzed and qualified and supplied to users as specified by the Government.

## 1.2 Sensor Description

A piezocable as used in this program (Figure 1) is a coaxial cable that includes a layer of flexible PVDF piezoelectric polymer material between the shield and center conductor. The PVDF is radially poled so that it produces an electrical response to the compressive strain produced by external pressure. Two types of piezocables are commercially available: one includes a piezo copolymer layer whereas the other includes spiral wrapped piezo film tape. These cables are manufactured in continuous lengths by Measurement Specialties, Inc. Both have a uniform sensitivity along their length. The voltage mode sensitivity is -92.5 dB $(V/Pa)^2$ and -94.2 dB $(V/Pa)^2$ for the copolymer and spiral wrap cables, respectively. Both have a charge mode sensitivity of 15 Pa/N. When operated in the voltage mode, appropriate spatial averaging can be achieved by selecting the cable length.

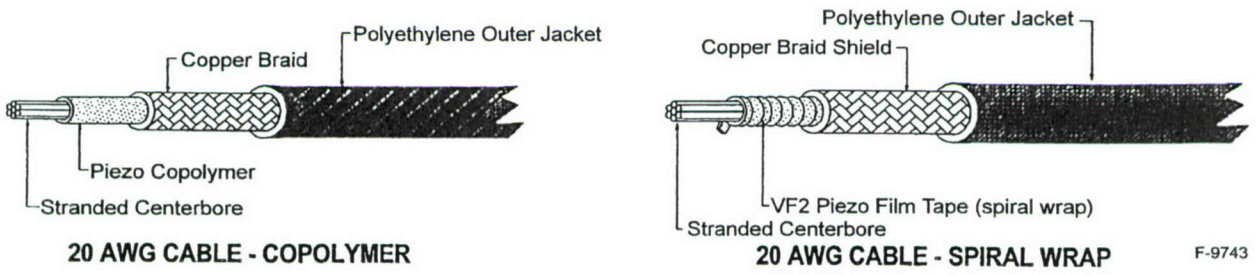


Figure 1. Two types of piezocable.

## 1.3 Anticipated Benefits

For application as an infrasound sensor, piezocable has been shown to offer several advantages:

- Direct electronic transduction
  - "speed of light" averaging over the sensor cable length
- Eliminates mechanical systems
  - multi-arm pipe averaging inlets and required support structures
  - manifolds and
  - microbarographs
- Enables novel enhanced performance options
  - signal processing options
  - noise reduction strategies
  - infrasound station geometries
- Environmentally robust
- Easily installed and reconfigured.

All-electric transduction and local processing allows a variety of options both in the array geometry and signal processing. A generic geometry is indicated in Figure 2. Geometric processing options are indicated in Figure 3. For example, if one arm of a multiple line array is anomalously noisy (for example due to an animal) that line can be ignored electronically. Or, consider a signal incident from the right as shown in the figure. The output from Cable lines A and B will be spatially filtered due to their projection in the direction of propagation, and thus higher frequency (shorter wavelength) components will be averaged out and appear to not exist. The signal on Cable C will not be spatially filtered at the higher frequencies, and a comparison with A and B outputs provides information that can be used to determine direction of incidence, perpendicular to Cable C in this case, because there will be greater levels of higher frequency sound detected. Table 1 provides a comparison of piezocable and microbarograph based arrays.

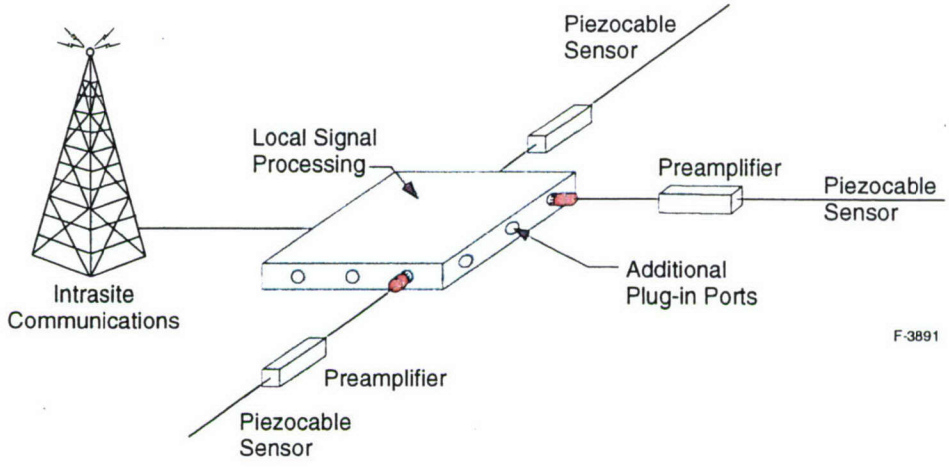


Figure 2. Piezocable sensor system concept.

***Independent Lines Enable Signal Processing Options***

1. **Quiet pair selection**
   Noise of pairs will depend on spatial correlations of wind noise; "steer" to identify quiet pair
2. **Dipole**
   Dipole consisting of A -E will have strongest signal response
3. **Eliminate noisy line**
   Ignore B until situation corrected
4. **Maximum sensitivity**
   Sum all (current option)
5. **Best lines selection**
   Choose lines with best signal to noise

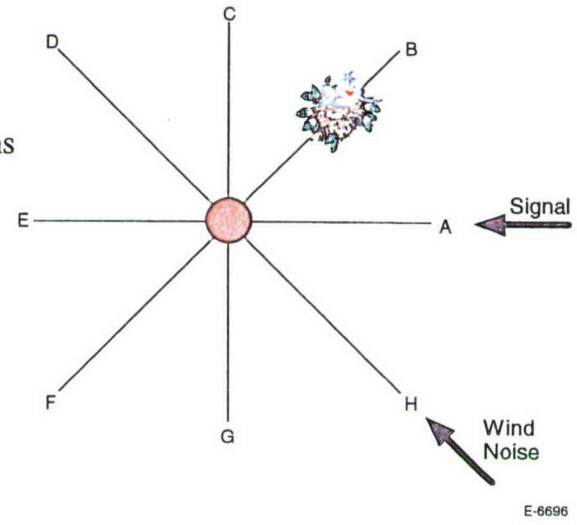


Figure 3. Signal processing options.

Table 1. Comparison with Standard Systems

| | Piezocable | Microbarograph Based |
|---|---|---|
| Transduction | • Cable generates electronic signal | Mechanical to electronic |
| Signals available | • Each cable line separately | Hoses/pipes summed in plenum; one output |
| Processing options | • Several alternatives possible | None |
| Noise specifications | • Cable and amplifier meet CTBT specifications | Meets CTBT specifications |
| Environmental sensitivities | • Deploy anywhere pressure can penetrate, e.g., under sand<br>• Fabricate with protections | Flow to transducer required; perforations susceptible to meteorology |
| Long-term stability and reliability | • No moving parts<br>• Materials stable in previous applications | Hoses have previously shown degradation |
| Maintenance | • Easily replaceable and inexpensive | Repair or replacement likely more difficult |
| Response to damage | • Self-diagnostics possible<br>• Electronically reconfigurable remotely or autonomously | Physical replacement |

## 2. Technical Description of the Program

### 2.1 Amplifier Development, Requirements and Description

One of the key enabling technologies for this system was the development of an extremely low frequency, low noise, high input impedance amplifier. After several iterations, a suitable design was achieved that also solved the apparently continuous very low frequency

current generation property of the piezo polymer cable materials, which prevented their use with charge coupling amplifiers.

The schematic for the amplifier is shown in Figure 4. Filter characteristics were chosen based on experience with the cable sensors and the desired frequency range of the IMS. The amplified gain characteristics are shown in Figure 5. The attenuation at very low frequencies minimizes the required dynamic range of the signal transmitter as well as draining off the low frequency current generation of the cables. Figure 6 provides photographs of four amplifiers and an autonomous operating timed signal injecting calibration source utilized in field experiments to monitor the condition of the amplifiers. A close-up of the signal generator is shown on the right side of the figure. Two amplifiers at a time were supplied with a ten second period square wave input signal, followed by the other two being excited after a minute with the same signal. This scheme avoided the situation of more than two sensors being overridden by the calibration signal at any time, incase an acoustic event were to occur during the signal injection period, usually set at once per day. By using a continuous square wave generator, the coherence between the two sets of sensors and amplifiers could also be determined when analyzing the amplifier outputs generated in response to the injected signals.

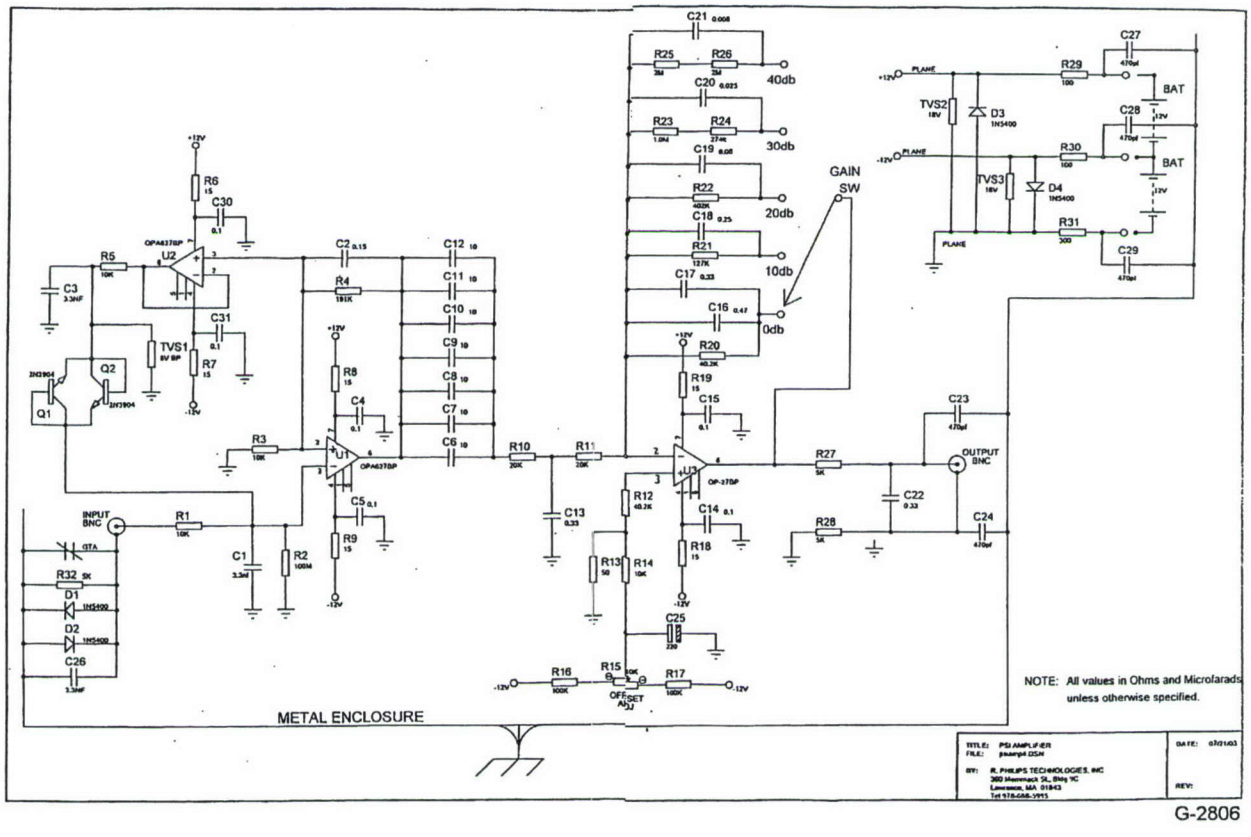


Figure 4. Circuit diagram for low frequency, low noise, high input impedance adjustable gain amplifier.

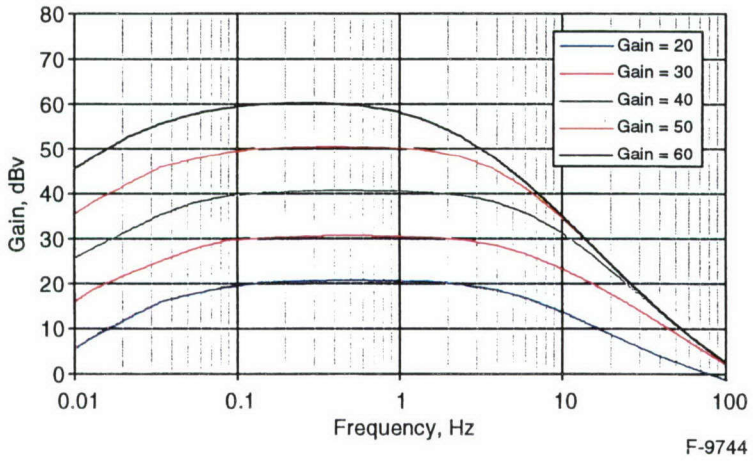


Figure 5. Amplifier gain for available maximum gain settings.

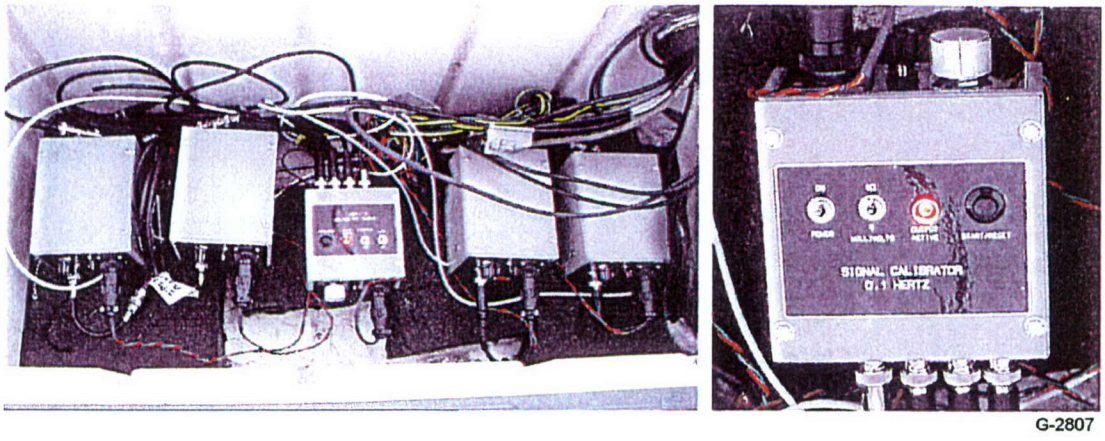


Figure 6. Four amplifiers and signal generator in weather resistant plastic container.

Once the amplifiers were fabricated, checked out and calibrated a variety of indoor and outdoor testing was accomplished. These tests included laboratory bench, PSI parking lot and ocean beach operations. A variety of configurations were evaluated including bare cables, thermally insulated cables, EM shielded cables and buried cables and various combinations of these. Acoustic calibration tests utilizing a simple controllable frequency low pressure source were also accomplished. Based on the results of this testing, the amplifiers were modified and a field testing configuration was defined. The signal generator that periodically generates a calibration square wave at the input to the amplifiers was used on each channel in the field tests to monitor performance and identify any problems that might have arisen.

The results of this testing identified two basic configurations that were tested at Pinon Flat Observatory. Thermally insulated buried cables were placed 3 to 4 in. under the ground surface and bare cables were placed 8 to 10 in. below the ground surface. Later at a test site at Kona Hawaii, the sensors were placed on the ground in the shaded area where there was little wind reported. Very limited data was obtained before the program period ended.

## 2.2 Basic Field Testing

Extensive testing of an array has been accomplished at Pinon Flat, CA. For these tests the cables were buried in trenches. Nine cables (seven 100 m and two 30 m) were installed as shown in Figure 7. (Note the proximity of the OFIS - another experimental sensor.) However only four could be used at any one time because of the limitation of the number of data telemetering channels that were made available to our program by UCSD. Power was provided by two 12 volt automotive type batteries that were readily kept charged by two flexible solar panels at the Pinon Flat Observatory site. Several photographs are provided in Figure 8.

The testing accomplished at Pinon Flat is summarized in Table 2. Several examples of the data are provided in Figures 9 through 13.

Figure 9 displays a typical acoustic signal. This signal was observed by three of our sensors as well as a microbarograph and the I57US pipe array. The data was filtered with a (0.7 to 2 Hz) bandpass to remove wind noise. Our two-sensor geometry allows an estimate of signal direction and speed. For this example the signal came from the southeast at 375 m/s (hence, not a seismic signal).

Figure 10 displays another acoustic event observed on three piezocables and the USCD microbarograph. As can be seen there is a multifeature event that is highly correlated across the four sensors. Two additional 100 m sensors were installed in the "New 100 m" transverse trench and have to be added to the figure information below.

Figure 11 displays data obtained from two piezocable sensors during a relatively quiet period, including the acoustic signals shown in Figure 10. The similarity between the sensor outputs for both signal and noise is as expected since these cables are directly next to each other in the trench. Also shown are the noise spectra for this period for these sensors and the nearby microbarograph (with noise reduction losses) measured in volts. Both signal sensitivity (from Figure 10) and noise (from Figure 11) of the piezocable sensors are about a factor of ten in magnitude (20 dB) smaller than in the microbarograph, indicating that the microbarograph and piezocable sensors have about the same signal to noise ratio.

Figure 12 displays how perpendicular piezocable sensors can be used to estimate direction. The fact that the 100 m N-S cable spatially filters the signal (i.e., there is substantially less higher frequency energy in the output from the N-S sensor than for the E-W sensor) implies that the signal was propagating nominally in a north/south direction.

Finally, Figure 13 displays a microbarom event. It was observed on two piezocables and the UCSD microbarograph. These pressures are believed to be produced by the interaction of storm waves with each other as waves breaking against the coastline of oceans. The predominant period is 5 seconds.

Figures 14 shows the USGS Earthquake Hazards Program first page of the December 22, 2003 earthquake in California, about 490 km from our sensors in Pinon Flat, and Figure 15 shows a plot starting (at left) at the time of the earthquakes 19:15:56 UTC and showing the approximately 68 seconds before the array cable sensors picked up the ground borne vibration arrival. This shows that these sensors, when buried a few inches below the surface, can pick up seismic as well as pressure signals.

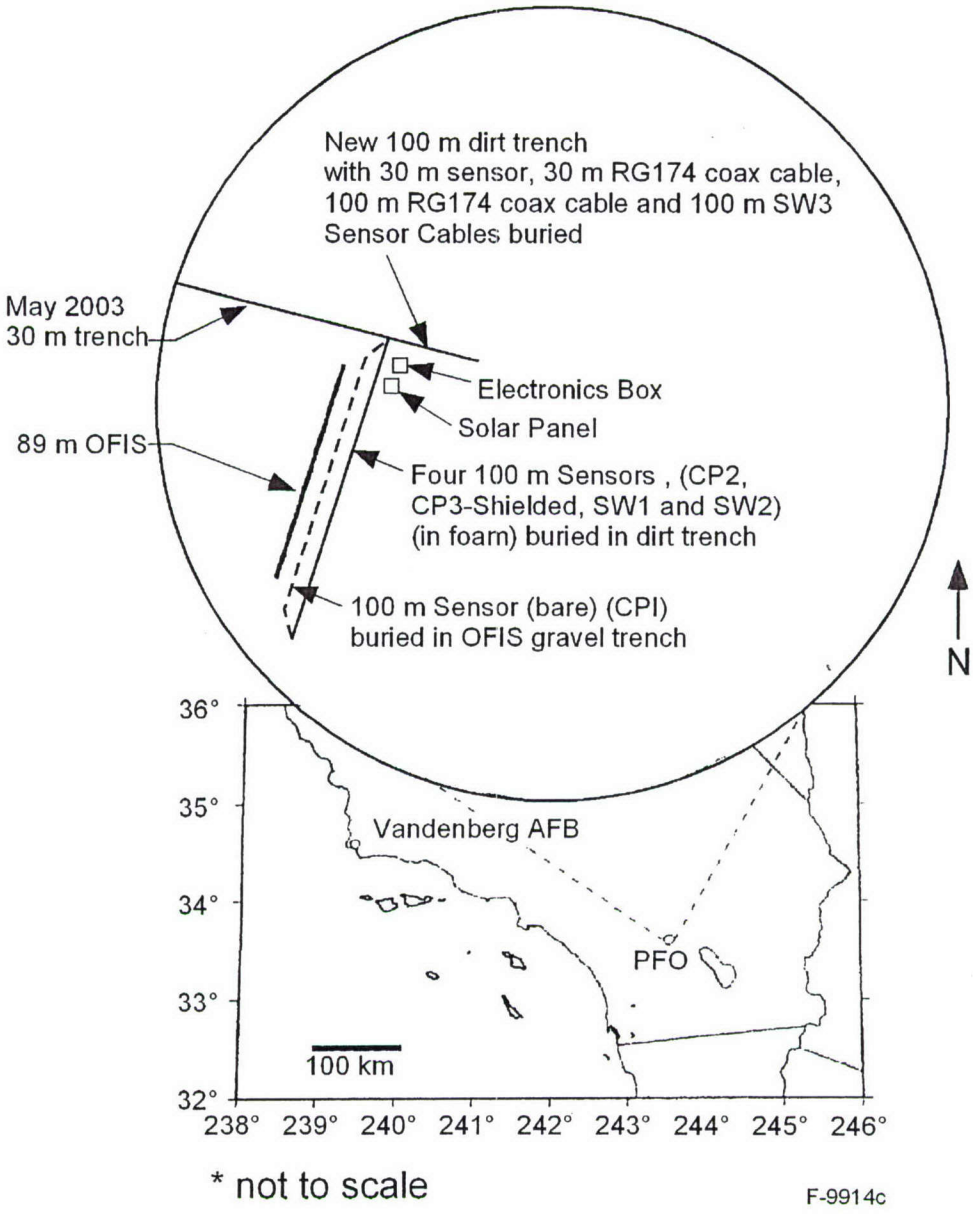


Figure 7. Piezocable infrasound sensor test station, Pinon Flat Observatory 157 US.

G-2808

Figure 8. Top row: partially and completely filled and smoothed trenches. Bottom row: container to left with four amplifiers and signal calibrator and to right box with one microbarograph. Also shown are solar panels used to provide all required system power to two 12-volt batteries in closed container. Right is the original north south trench shown before being refilled (next to the black plastic covered OFIS array).

Table 2. Pinon Flat Observatory Testing

| Test | Results | Conclusions |
|---|---|---|
| 1. Tested four 100 m cables (SW and CP) in thermal foam on 2 ft spool. | • Excellent agreement in amplitude and phase | • Cables and amplifiers working as anticipated |
| 2. Tested 100 m cables uncoiled next to OFIS. | • High noise levels lead to amplifier saturation and dropouts in windy conditions | • Need to bury cables to minimize wind noise |
| 3. Installed and tested four 100 m cables in PSI's trench, buried 4 to 6 in. deep in thermal foam and one 100 m cable 2 in. deep in trench next to trench with four cables. | • Greatly reduced noise<br>• High coherence between cables<br>• AMP3 out of phase with others at times<br>• Sensitivity seems to vary among sensor/amplifier pairs | • Burying cables effective against wind-generated noise in trench<br>• Residual noise similar on all buried sensors |
| 4. Reinstalled and tested 100 m cable in OFIS gravel trench | • Higher noise observed | • Shallow burial in gravel less effective against wind-generated noise |
| 5. Installed and tested 30 m cable in second PSI trench, buried 1 to 2 in.<br>Trench at right angle to PSI's first trench and OFIS trench. | • Noise coherent with other sensors<br>• Higher frequencies observed in 30-m output | • Residual noise similar to other sensors<br>• 100 m cables provide more spatial averaging as anticipated |
| 6. Installed two 100 m cables in extended second trench. | • Sensors very noisy in open trench<br>• Filling trench reduced noise by about 50 dB | • Experience in previous trench repeated |
| 7. Observed Central California earthquake via ground borne vibrations from about 450 km distance. | • Sensors of both types, SW and CP, observed similar time trace signals. Even though the North-South sensors were in the thermal isolation tubing, their signal levels were higher. | • The sensitivity of the sensors indicated that the more perpendicular to the seismic signal, the larger the signal. Travel speed was about 7.25 km/s. |

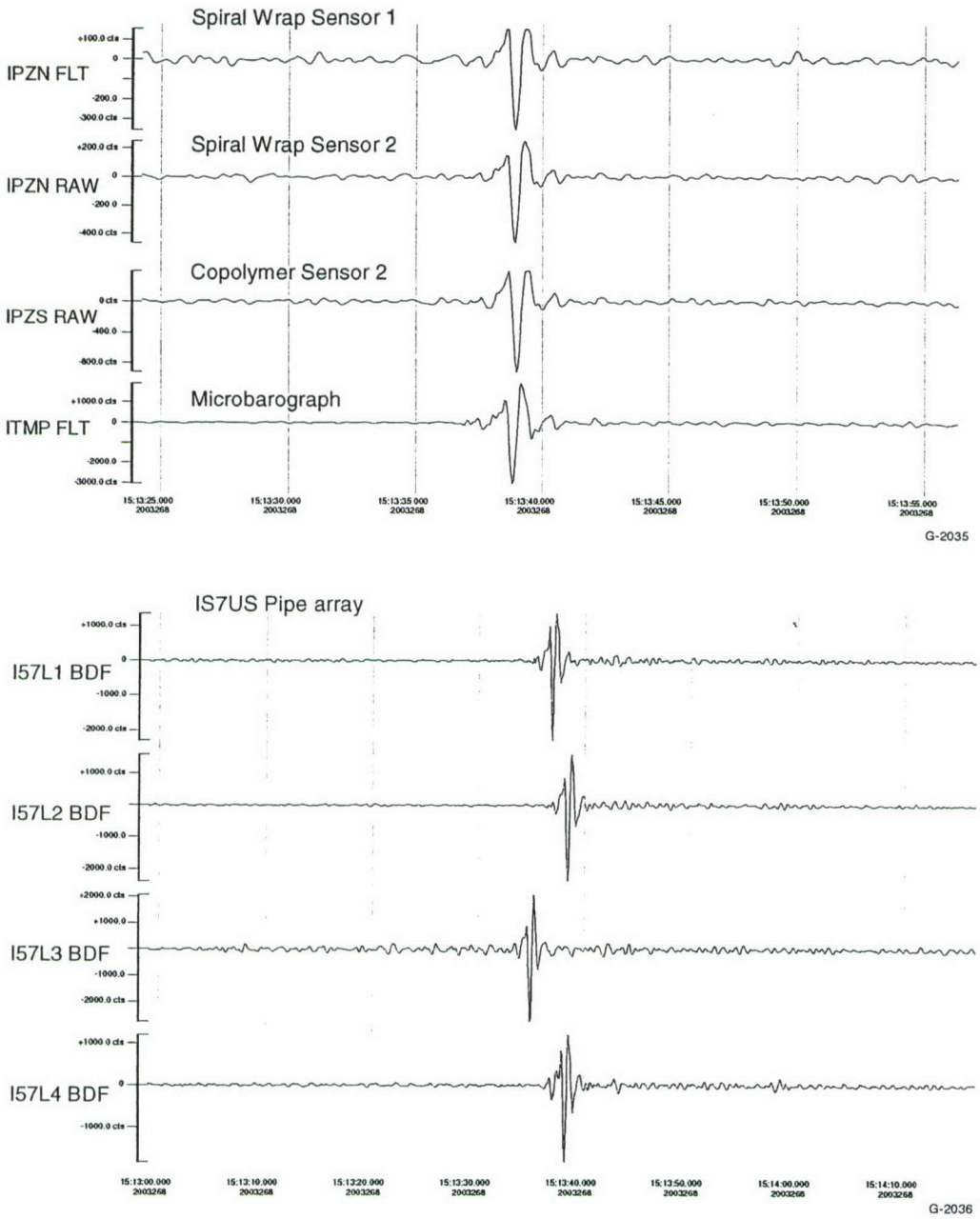


Figure 9. Examples of "acoustic events" measured using piezo polymer sensors (top) and current microbarograph-based sensors (bottom).

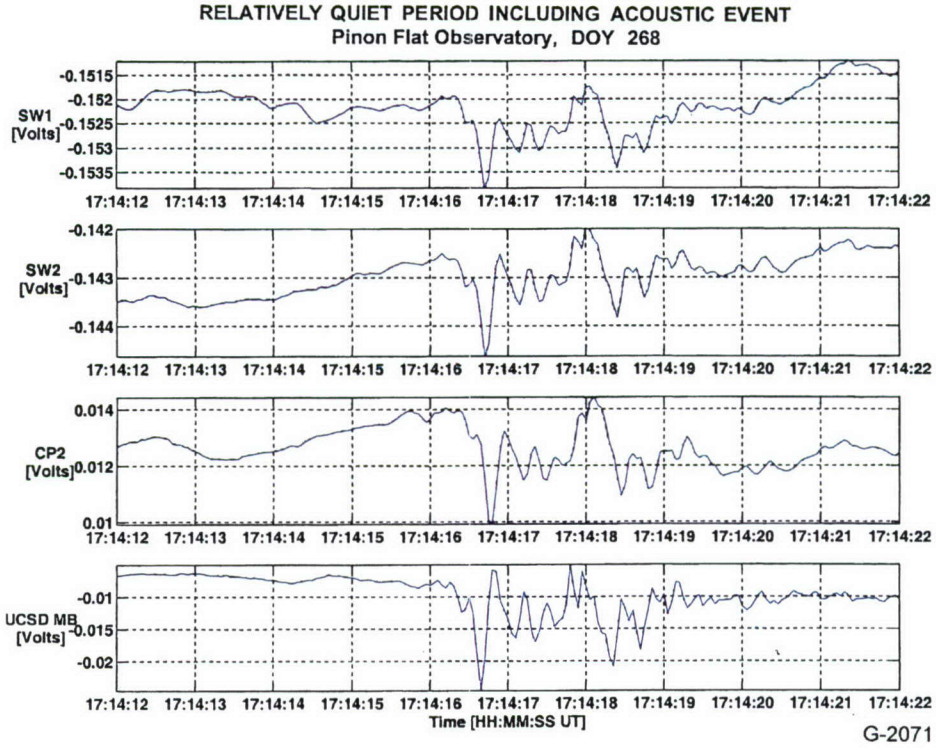


Figure 10. "Acoustic event" recorded by three cables and 1 microbarograph sensor.

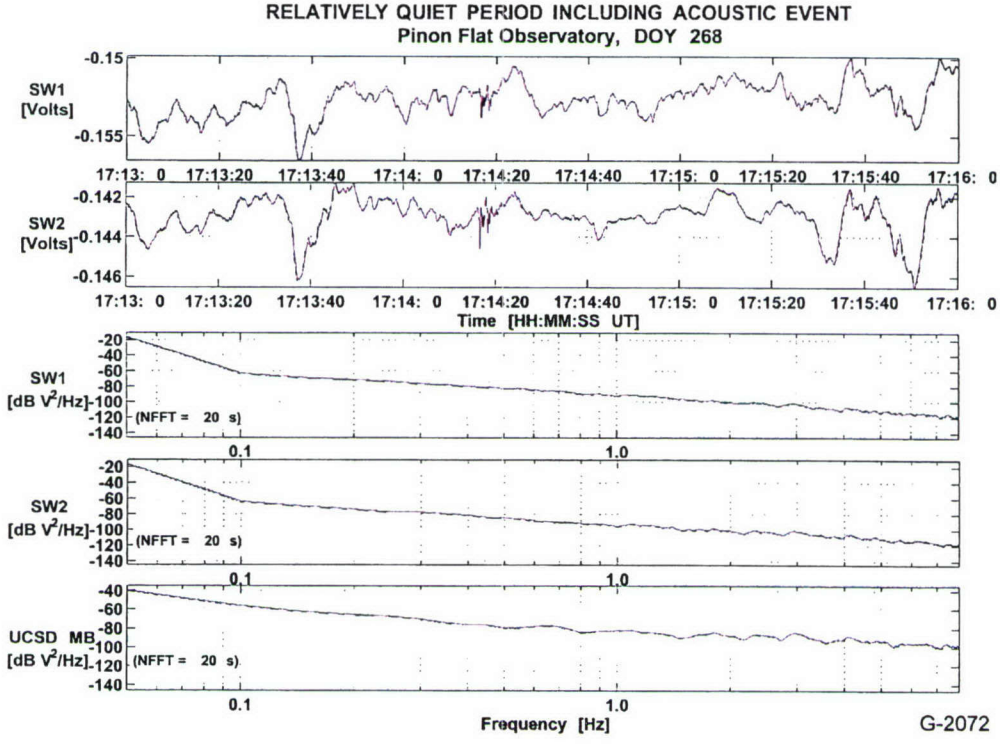


Figure 11. Longer time trace of data from previous figure also showing spectra of noise over the entire period.

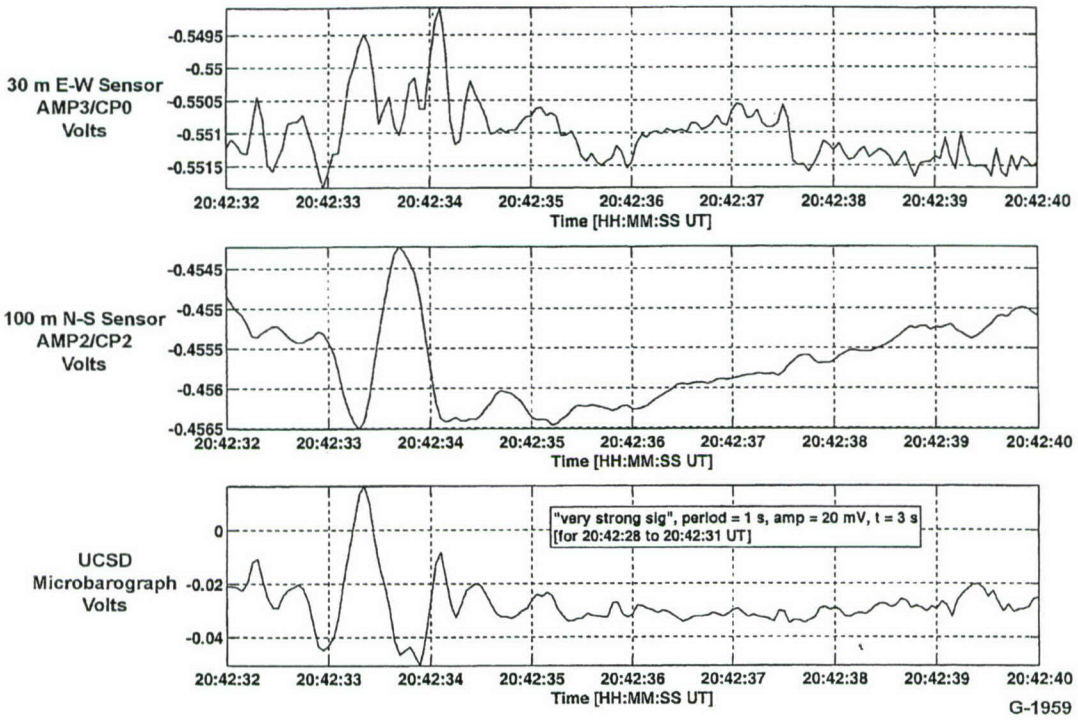


Figure 12. Time traces from North-South and East-West cables plus microbarograph signal.

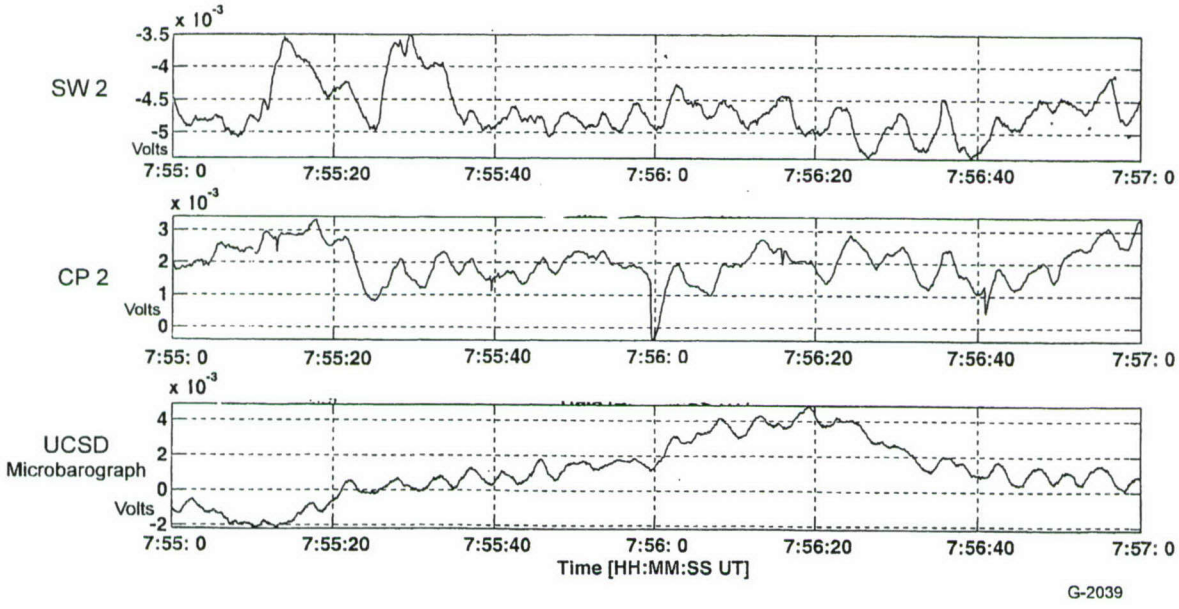


Figure 13. Microbarom pressures (about 5 second periods) as measured by three cable sensors and a reference microbarograph.

USGS
Earthquake Hazards Program

Latest Quakes

HOME | ABOUT US | EQ GLOSSARY | FOR TEACHERS | PRODUCTS & SERVICES | DID YOU FEEL IT? | FAQ | SEARCH

Earthquake in the News

Magnitude 6.5 - CENTRAL CALIFORNIA
2003 December 22 19:15:56 UTC

004356

Current Earthquakes

USA
World

NEIC Current Earthquake Information

ShakeMaps

Seismogram Displays

Past & Historical Earthquakes

Earthquake Notification E-mail

Pinon 33.61°N 116.5°W ~ 490Km away

**Preliminary Earthquake Report**
U.S. Geological Survey, Menlo Park, California
U.C. Berkeley Seismological Laboratory, Berkeley, California

A strong earthquake occurred at 19:15:56 (UTC) on Monday, December 22, 2003. The magnitude 6.5 event has been located in CENTRAL CALIFORNIA. The hypocentral depth was estimated to be 8 km ( 5 miles). (This event has been reviewed by a seismologist.)

Magnitude **6.5**

Monday, December 22, 2003 at 19:15:56 (UTC)
= Coordinated Universal Time
**Monday, December 22, 2003 at 11:15:56 AM**
= local time at epicenter

35.706°N, 121.102°W

Depth 7.6 km (4.7 miles)

Region **CENTRAL CALIFORNIA**

Distances 11 km (6 miles) NE (49°) from **San Simeon, CA**
17 km (10 miles) N (356°) from **Cambria, CA**
20 km (13 miles) W (260°) from **Lake Nacimiento, CA**
39 km (24 miles) WNW (283°) from **Paso Robles, CA**
195 km (121 miles) SSE (158°) from **San Jose City**

G-4025

Figure 14. USGS preliminary earthquake report.

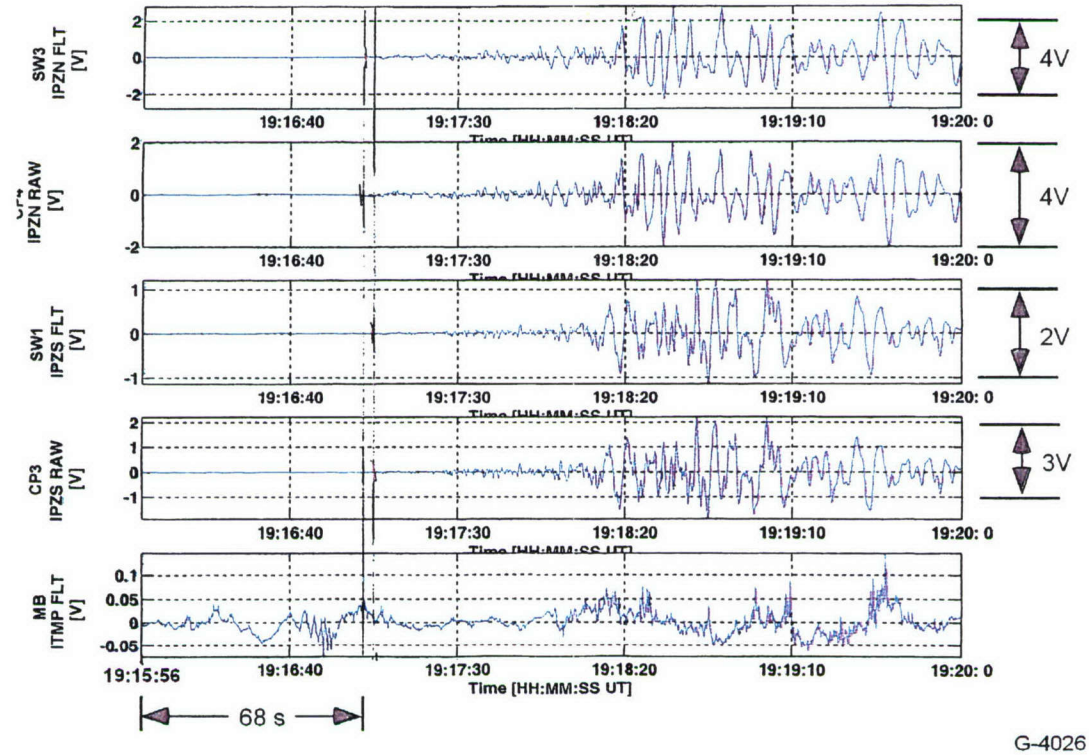


Figure 15. Response of arrays to earthquake 490 km away.

## 2.3 Detailed Testing at Pinon Flat Observatory

### 2.3.1 Configurations

Background noise for piezocables and the reference microbarograph were studied in detail for periods representing two configurations at the Pinon Flat Observatory. These were the final configurations planned for the Observatory and represent the culmination of this program.

#### 2.3.1.1 Configuration 1

This configuration was completed on 31 October 2003, DOY 304. During this period the East-West Trench was dug and piezocables SW3 and CP4 were installed in it. Unfortunately, there was insufficient time to completely fill in the trench, and about half of these new sensors were left uncovered. In the North-South trench, piezocables SW1 and CP2 were connected. All amplifiers appeared to working properly when the site was left. Good signals were obtained from all sensors except CP2.

#### 2.3.1.2 Configuration 2

Completed on 7 December 2003, DOY 341, this configuration represents the complete demonstration system for a perpendicular line infrasound sensor system. Both trenches are filled in and smoothed on the top to minimize wind excitation. In the North-South trench, sensors SW1 and CP3 (which is sheathed in a conducting braid) were connected, and in the East-West trench, SW3 and CP4 were connected. All amplifiers appeared to be working normally when the site was left.

## 2.4 Methods

### 2.4.1 Data Selection

A brief study of the noise data was necessitated by contractual time limitations. Data for certain representative days were downloaded and divided into daily, 1- and 2-hour segments, and 15 min segments. The latter were used as the main subjects of analysis, since these correspond with the standard noise measurement intervals. Each day was characterized by twenty-four 15-min noise spectra taken as close to the hour as possible. Time traces for these intervals were first inspected for the presence of spikes, which tended to raise the spectra several dB over most of the bandwidth of interest. These spikes are readily identified and not likely to be erroneously identified as signals and it is judged that they should not be considered part of the system noise for the purpose of estimating receiver operating characteristics. Consequently, only spike-free intervals were taken to represent the background noise of the sensors. For a small number of hours, finding spike-free 15 min intervals was difficult and in some cases not possible. These hours were either skipped or somewhat shorter intervals were taken. Almost all noise comparisons to be made here are at 1 Hz, which was selected as a frequency representative of many of the signals observed.

### 2.4.2 Wind Characterization

Each 15-min interval was also characterized by a wind velocity and direction obtained by inspection of the time histories of the UCSD reference wind sensor supplied in the IPZN telemetry channel. These values taken represent an "eyeball" estimate of the median values of speed and direction (measured from 0 to 4 V) for each 15-min interval. This very approximate method obviously contributes to scatter in some of the noise vs windspeed plots.

## 2.5 Lowest Noise Observed

As expected, the quietest periods observed on the piezocable and microbarograph (MB) sensors were during periods of least wind. Data for a quiet period, DOY 351 9:0:0 to 9:15:0, is shown in Figures 16(a), 16(b), and 16(c). Figure 16(a) shows the wind velocity and direction measured on the two wind sensors. The median wind speed voltage is about 0.01 volts, corresponding to a wind speed of about 1 mph. Wind direction is from the North. Data at this condition is inherently interesting in that it characterizes the noise floor of the instruments. It also illustrates some universal characteristics of the data.

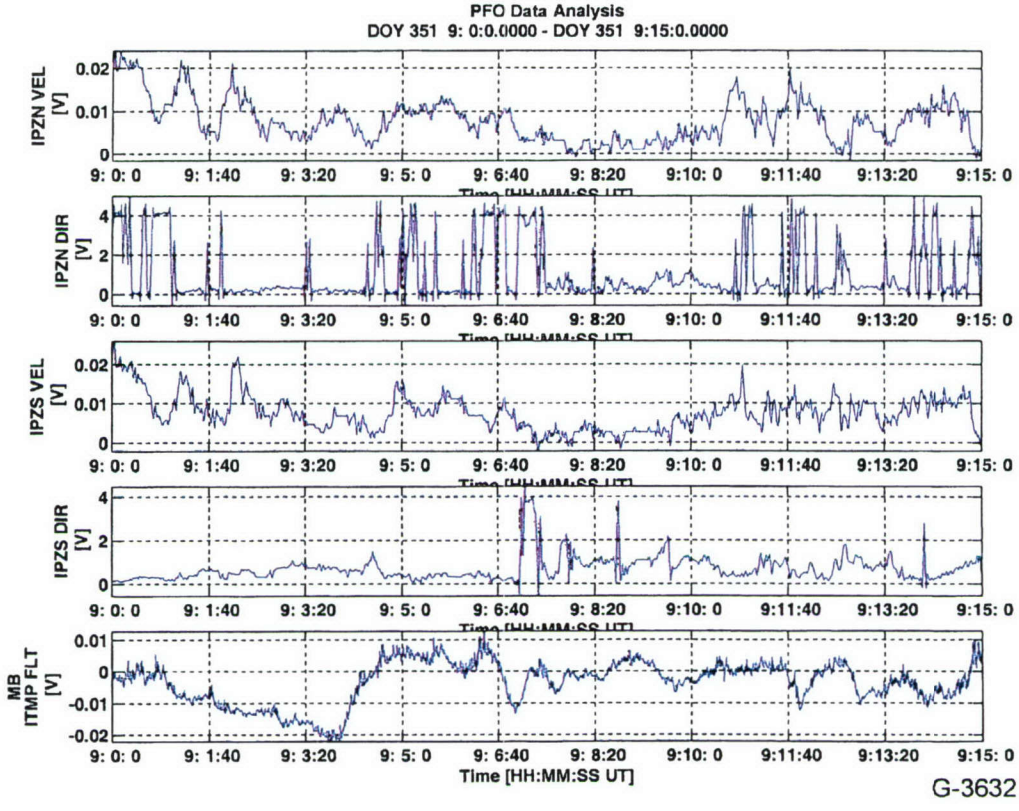


(a) Wind velocity and direction from two sensors and microbarograph pressure

Figure 16. 15 min of time and sensor signal data from 17 December 2003 (DOY 351) and spectral analysis of the sensor signals.

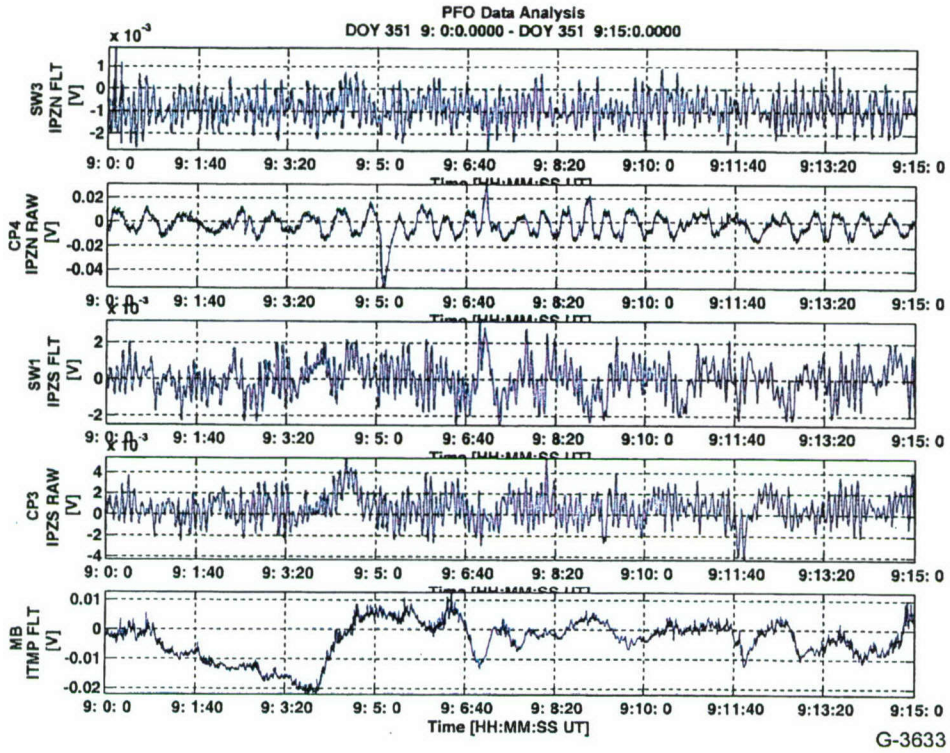


(b) Time signals from four cable sensors and microbarograph (bottom)

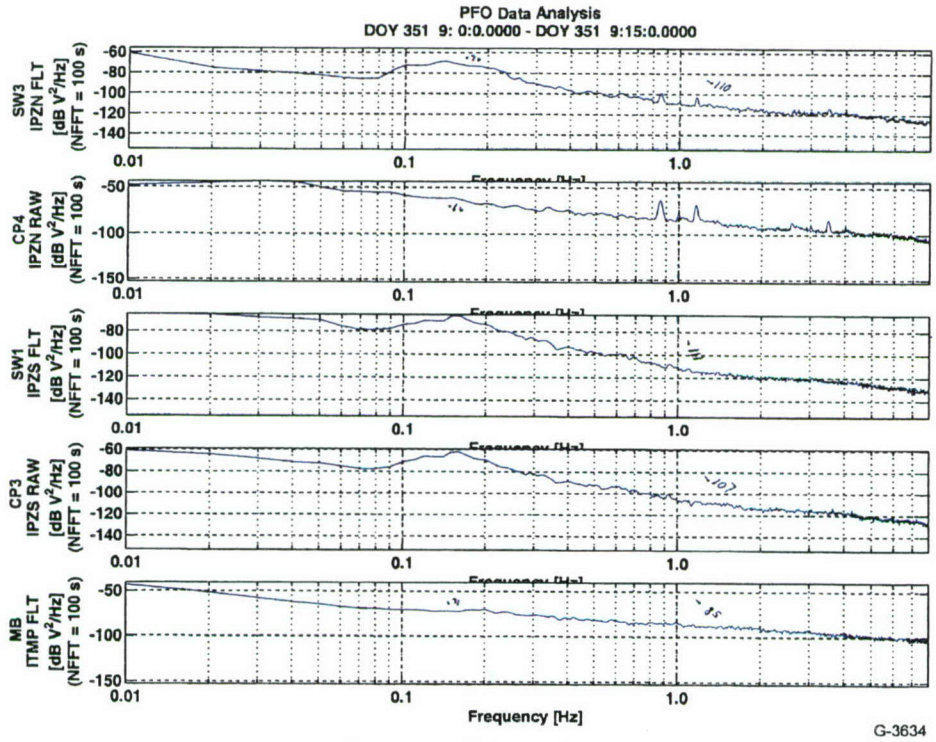


(c) Spectra of time signals

Figure 16. (Continued) 15 min of time and sensor signal data from 17 December 2003 (DOY 351) and spectral analysis of the sensor signals.

Time histories for SW3, CP4, SW1, CP3 and the microbarograph are shown on Figure 16(b). Very clean regular signals with peak to peak amplitudes on the order of a few millivolts are observed on SW3, SW1 and CP3, which are almost certainly due to microbaroms. The time trace for CP4 displays larger variability at lower frequencies making it difficult to identify microbarom-like signals. Likewise, microbars are not clearly visible on the microbarograph time trace.

Noise spectra for four piezocables and the microbarograph are shown in Figure 16(c). These spectra have a bin width of 0.01 Hz and bandwidth of 0.015 Hz. To convert to spectrum level (db re 1 $V^2$/Hz) -- 10 log (0.010) = 18.2 dB must be added to these levels. Conversion to pressure spectrum level, dB re $Pa^2$/Hz, requires addition of the sensitivity calibrations 54.2 dB re $Pa^2/V^2$ for the SW cables and 52.5 dB re $Pa^2/V^2$ for the CP cables. Spectra for SW3, SW1 and CP3 show microbarom peaks around 0.13 to 0.15 Hz with levels -70, -60, and -62 dB, corresponding to pressures on the order of 0 to 10 dB re 1 $Pa^2$/Hz. Levels at 1 Hz are 45 to 50 dB lower, or around -40 dB re 1 $Pa^2$/Hz.

These spectra also demonstrate that the noise in the piezocables above 1 Hz drops more rapidly with frequency than that in the microbarograph. By 8 Hz, the former (with the exception of CP4 which contains electronic noise) have fallen below -120 dB re 1 V whereas the latter is barely below -100 dB. This difference above 1 Hz is common in almost all the data observed.

While the power spectrum for CP4 does not show a pronounced peak at the microbarom frequency, it is at a comparable level (about -10 dB), indicating that it may be receiving microbarom energy along with other contributions in this range. In fact, a spurious noise component most likely due to an unknown electronic problem had been noted on CP4 during a quick look analysis of this sensor. This phenomenon is indicated by the two spectral peaks on either side of 1 Hz. It apparently contributes to the overall noise of CP4 as well as at these two frequencies and for this reason CP4 is not considered a reliable sensor. It is somewhat interesting to note that there are smaller versions of these peaks about 1 Hz in SW3 which shares a telemetry channel with CP4, indicating that some of this likely electronic energy is bleeding through to SW3 when the latter is in as quiet a state as it is during this time period. Fortunately, this phenomenon is a small factor in SW3 and is not typically observed at other times in this sensor.

A pronounced microbarom peak is not observed in the MB power spectrum, which has a value of about -71 dB at 0.13 Hz, representing pressure levels 30 dB below that in the piezocables according to the nominal sensitivities for the two types of sensors. This discrepancy has been noted consistently in the analysis of piezocable data but it has not been satisfactorily explained. A rolloff in the frequency response in the MB electronics could account for this difference, but to our knowledge this does not exist. An enhanced sensitivity of piezocables to infrasound at microbarom frequencies could explain this discrepancy. This could occur, for example, if there is a substantial ground motion in response to airborne pressure fluctuations at these frequencies. A comparable discrepancy does not appear at higher frequencies when acoustic events are simultaneously detected by piezocable and MB sensors with both sensor types recording practically the same amplitude signals.

## 2.6 Configuration 1

### 2.6.1 Overview

Time traces for DOY 309 22:52:00 to 23:07:00 showing the four piezocables connected in this configuration, CP2, CP4, SW1 and SW3, and the microbarograph are shown in Figure 17. The range of voltages among these curves is quite large. SW1 and the MB are a few mVpp, CP2 is on the order of 2 Vpp, and the voltages for CP4 and SW3, the piezocables in the "open" East-West trench, are on the order of 20 Vpp. These large voltages indicate that the noise in the open trench is on the order of 60 dB larger than for the buried SW1and clearly demonstrate the need for burial. CP2 is also quite noisy, only about 20 dB quieter than the open trench, most likely indicating a severe malfunction in this sensor.

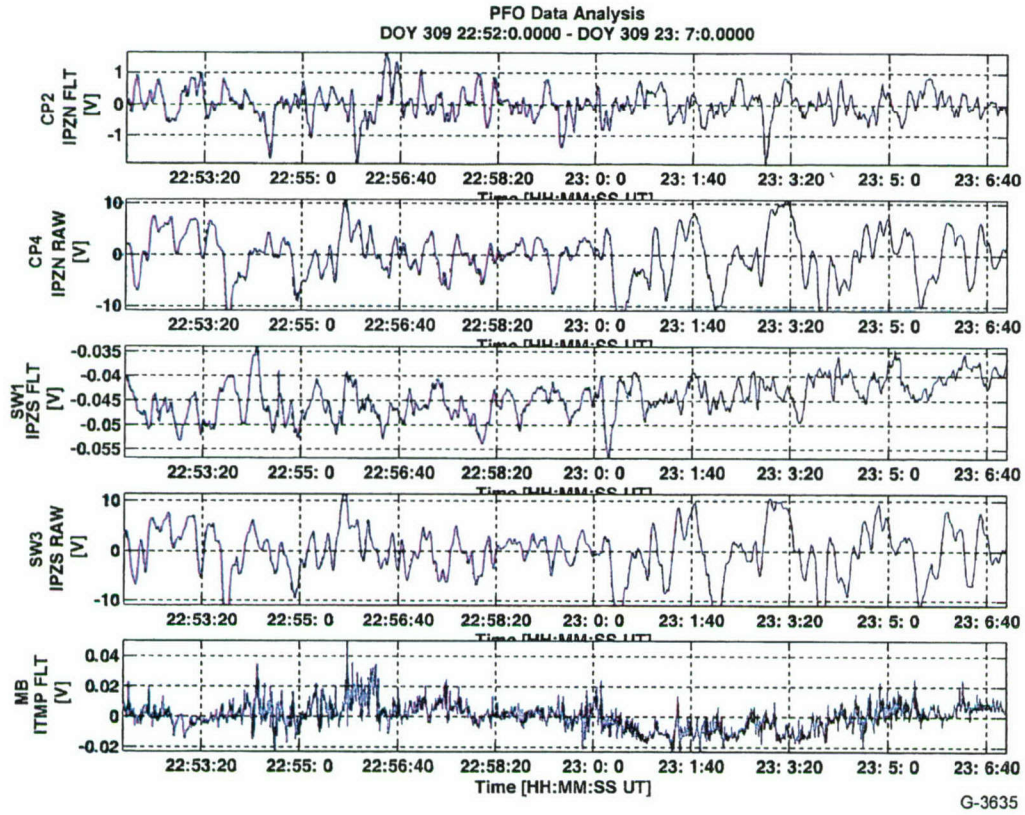


Figure 17. Signal time traces from DOY 309.

SW1 and MB are consistent with each other, and apparently working normally. That they appear to have about the same level may seem confusing, as the sensitivity of the microbarograph is about 20 dB greater than that of the piezocables, but not when the frequency components of the spectra are considered. The MB signal is here dominated by 1 Hz noise, which is much weaker in the piezocables.

From these and similar data it is clear that in this configuration the only sensors that are providing useable data are SW1 and MB. In configuration 2, with the trench filled in, performance of SW3 and CP4 approach that of SW1 (although as shown above CP4 had an electronic problem.) No explanation for the high voltages in CP2 was found, and this sensor was not used again.

### 2.6.2 A DOY 309 Acoustic Signal Event

Figure 18 shows a signal detected by SW1 and MB on DOY 309. Beginning around 23:50:45 and lasting 10 to 15 seconds, this signal has frequency content in the range 1.5 to 2 Hz. The voltage signal in SW1 is on the order of a factor of 10 lower than that of the micro. barograph, which is consistent with the sensor sensitivities. The signal in the MB appears to include some higher frequency energy but this could simply be due to MB noise. The general upward trend in the signal with time is actually comparable for the two sensors even though it appears much bigger in the SW1 signal, which is plotted on a smaller coordinate scale.

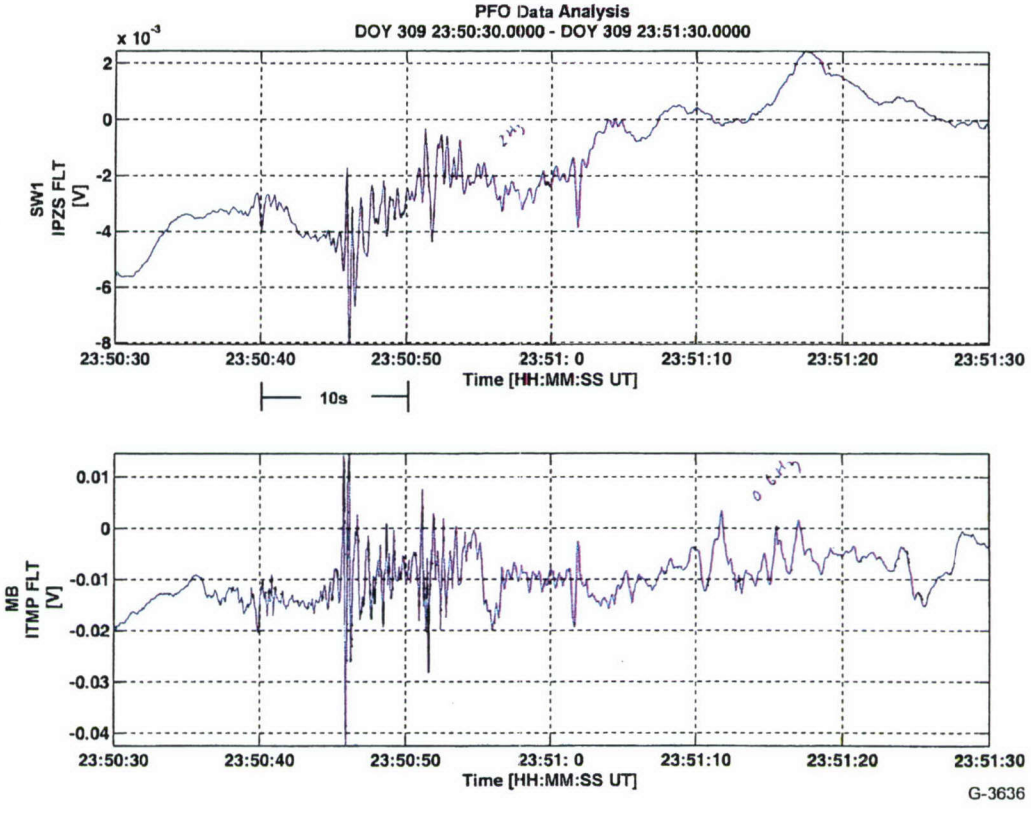


Figure 18. Acoustic event signals from cable SW1 and the microbarograph.

### 2.6.3 Microbarograph 1 Hz Noise Wind Response

During the period after the installation of this configuration, the sensitivity of the microbarograph to wind noise changed. As will be shown in the next section, between DOY 307 and 308 the noise in the MB near 1 Hz increased significantly. Figure 19 demonstrates the "high" state of response. This figure shows the wind speed and direction as measured by two sensors and the MB signal. The clearest example of wind-generated noise is at 21:46:40 where wind speed increases rapidly from about 3 mph to about 11 mph and the character of the MB output changes abruptly as the energy in the range 0.5 to 1 Hz increases dramatically. Quieter periods associated with lower wind speeds are seen near 21:53:20 and more obviously at 21:56:40.

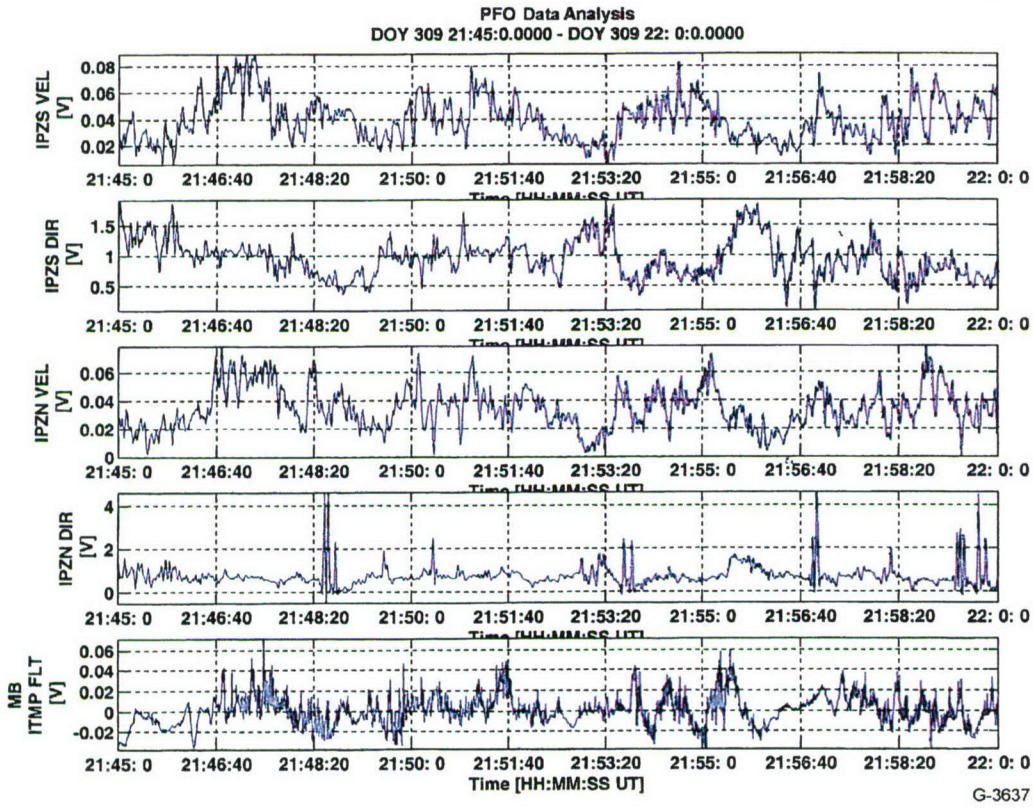


Figure 19. Microbarograph noise and wind speed and direction data showing increase starting at 21:46:40.

While the origin of change in sensitivity is unknown, the event shown in Figure 20 may be related, especially since all data taken after this time shows the higher sensitivity. This figure shows the time trace output of SW1 and MB between DOY 308, 0:58:00 and 1:12:00. At about 1:1:18 there is a large glitch in the MB output followed by a smaller feature at about 1:1:40. There is a great increase in the higher frequency content of the MB signal after this event. Almost simultaneously, there is a small glitch in SW1 a few seconds after the large glitch in MB followed by a large spike (to the amplifier rail) at about 1:1:55. No events are known to have occurred at this time, but it is clear that something caused large responses on both sensors and may have altered the behavior of the microbarograph.

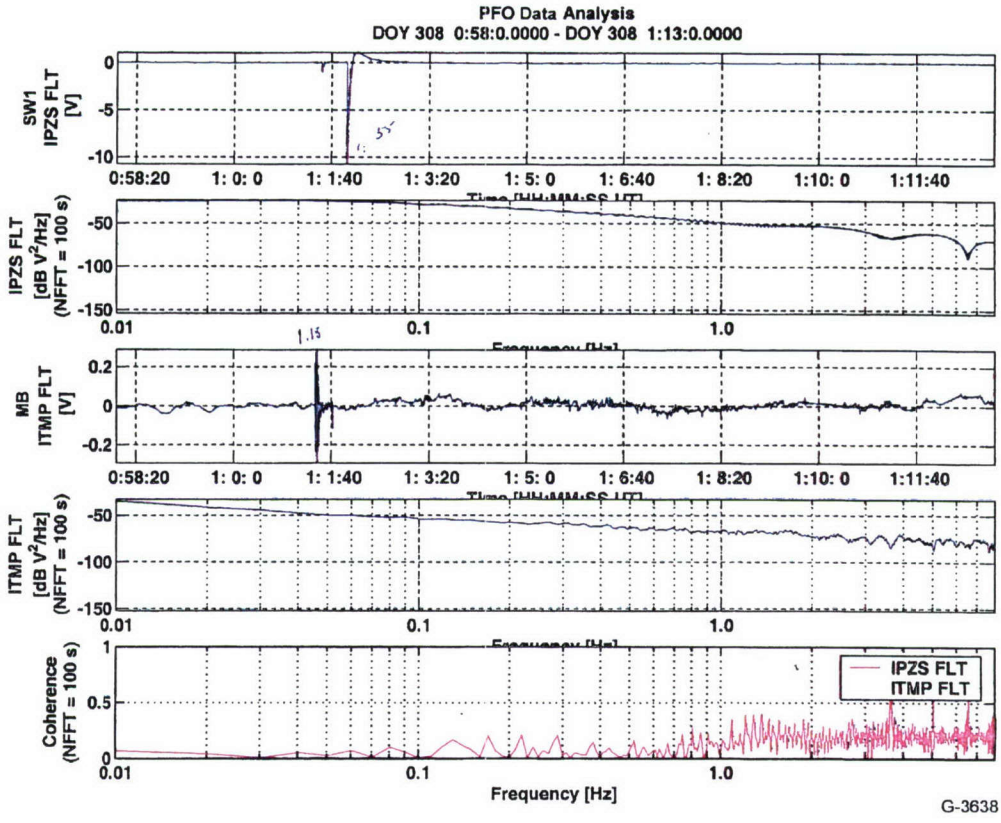


Figure 20. Time trace data for SW1 and the microbarograph showing event at 1.15 followed by increased MB noise. Spectral response shown in second and fourth curves, along with coherence at bottom.

### 2.6.4 Comparisons of SW1 with Microbarograph

#### 2.6.4.1 DOY 309

This was a relatively quiet day. Figure 21 traces the absolute noise power dB re 1 $Pa^2$ in 0.01 Hz bins (~0.015 BW) at 1 Hz for 15-min data samples as a function of time. From 0:0 to about 17:00 UT, the noise of the MB remained about 5 to 10 dB greater than that of SW1. At 15:00, the wind was particularly light and the MB signal was very low, about 7 dB below that of SW1. However, at around 18:00 and later, as the wind picked up, both sensors became noisier, with the microbarometer noise rising to about 10 to 15 dB above SW1. This is demonstrated more clearly in Figure 22 which plots noise at 1 Hz for this day as a function of wind speed. This again shows the extremely low noise floor of the microbarograph at the lowest wind speed, the 5 to 10 dB advantage of SW1 at light winds, and a 10 to 15 dB noise advantage for the SW1 at speeds from 3 to 5 mph.

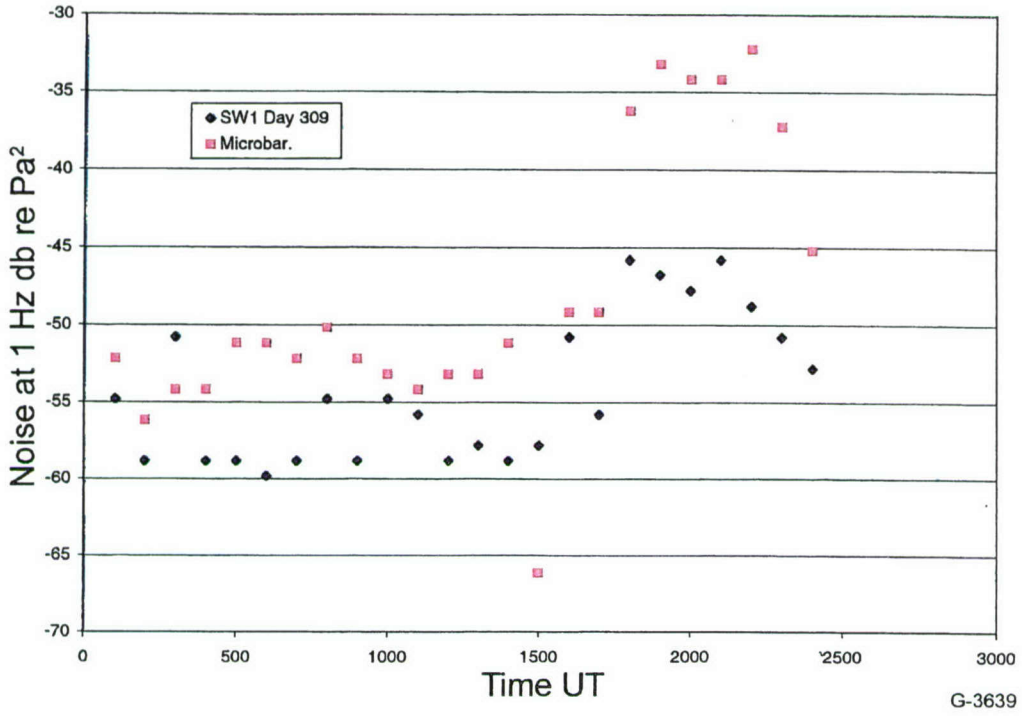


Figure 21. 1 Hz noise of SW1 and MB for 15 min average during DOY 309 showing lower signals from SW1 indicating the 5 to 10 dB benefit of length averaging in light winds.

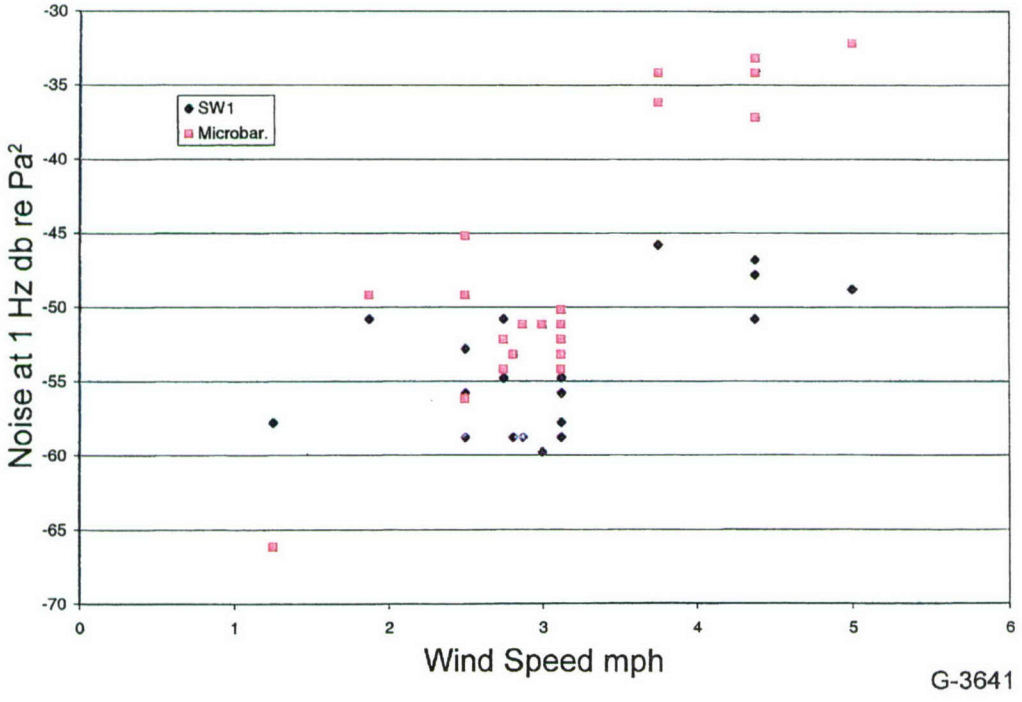


Figure 22. 1 Hz noise of SW1 and MB for 15 min average during DOY 309 showing lower signals from SW1 indicating the more substantial benefit, 10 to 15 dB, of length averaging in moderate winds, above 3 mph.

2.6.4.2 DOY 307 and 308

Figure 23 is a plot of noise at 1 Hz for SW1 and MB for 2 days with a range of wind speeds up to 18 mph. For the lightest winds, below 4 mph, the microbarograph is quieter by up to 10 dB as was noted with data from DOY 309. During DOY 308, for winds from 4 to 12 mph, the microbarograph was about 5 to 10 dB noisier than SW1. However during day 307 in this windspeed range, the microbarograph was about 5 to 10 dB quieter than SW1. This difference is due to a significant increase in microbarograph wind noise sensitivity at 1 Hz between days 307 and 308. A 7 to 10 dB advantage of the microbarograph or DOY 307 is also observed at 14 and 18 mph.

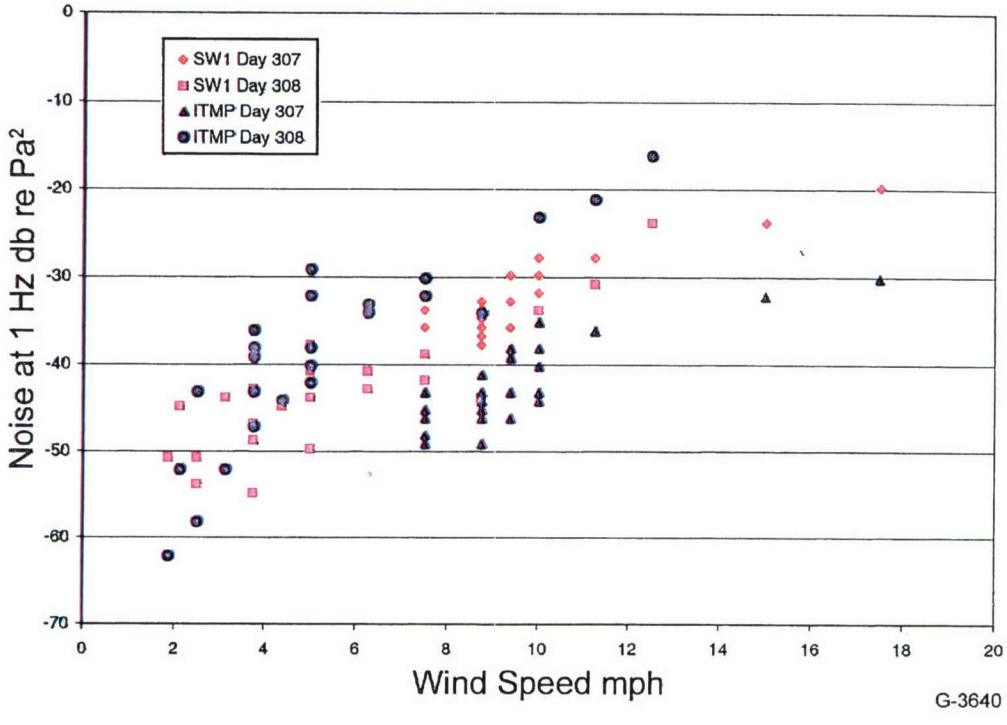


Figure 23. Averaged noise levels at 1 Hz for SW1 and the microbarograph.

For completeness, the noise vs wind speed for DOY 309 is replotted in Figure 24 to allow direct comparison with Figure 23, which comparison shows that the data taken on these 2 days are consistent.

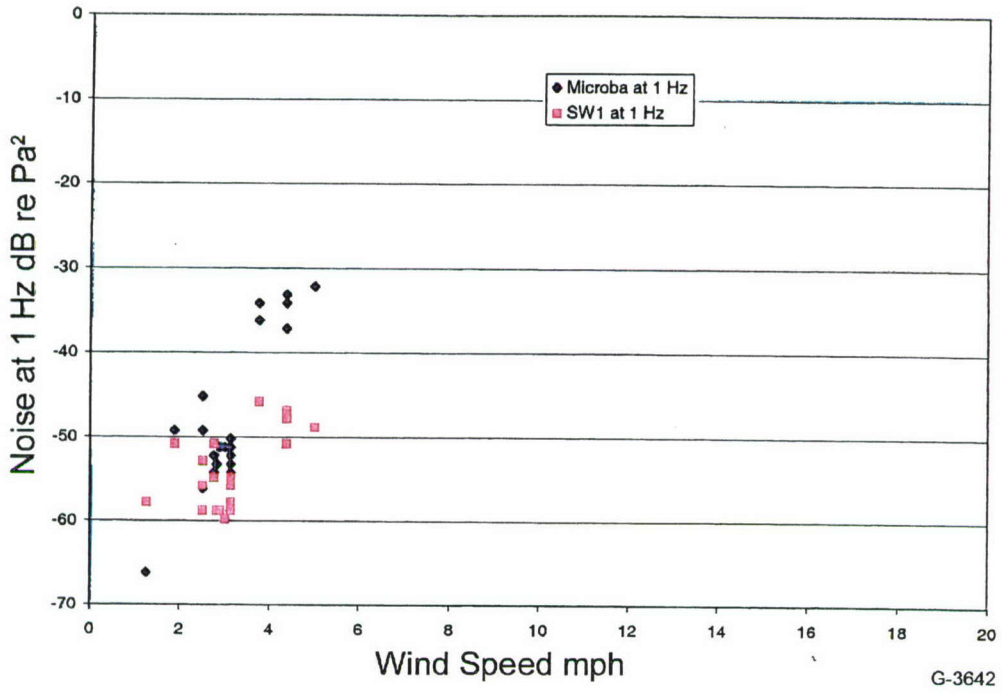


Figure 24. Noise level vs wind speed at 1 Hz for SW1 and the microbarograph for DOY 309.

## 2.7 Configuration 2

### 2.7.1 Overview

In this last configuration, piezocables in both perpendicular directions, properly buried, were active. In the North-South trench, SW1 and CP3 were connected, with SW1 the more reliable sensor. In the East-West trench, SW3 and CP4 were active, although CP4 was plagued by an electronic problem.

### 2.7.2 Day 352 – A Low Wind Example

Figure 25 summarizes the 1 Hz noise data for SW3, SW1, CP3 and the microbarograph during DOY 352. Here, for speeds below about 2.5 mph, the noise levels are about the same. For wind speeds 2.5 mph and above occurring after 2000, the piezocables are 10 to 15 dB quieter on average. These levels are entirely consistent with those shown in, for example, Figure 23 for DOY 308 (the "higher" noise level for the microbarograph).

A direct comparison between SW1 and SW3 is shown in Figure 26, showing the difference in dB between the two sensors at 1 Hz as a function of wind speed for wind from the North and from the East. For both wind directions, the difference is positive for all data points up to 4 mph, suggesting that (a) SW3 is typically up to 5 dB quieter than SW1, and (b) wind direction is not a factor. This first conclusion may be due simply to the fact that SW3 is buried deeper in its trench than SW1 by about 9 in. This also suggests, since SW1 is embedded in a foam jacket to minimize thermally-induced noise, that the thermal jacketing is not highly effective, and that burying is a more important noise control feature.

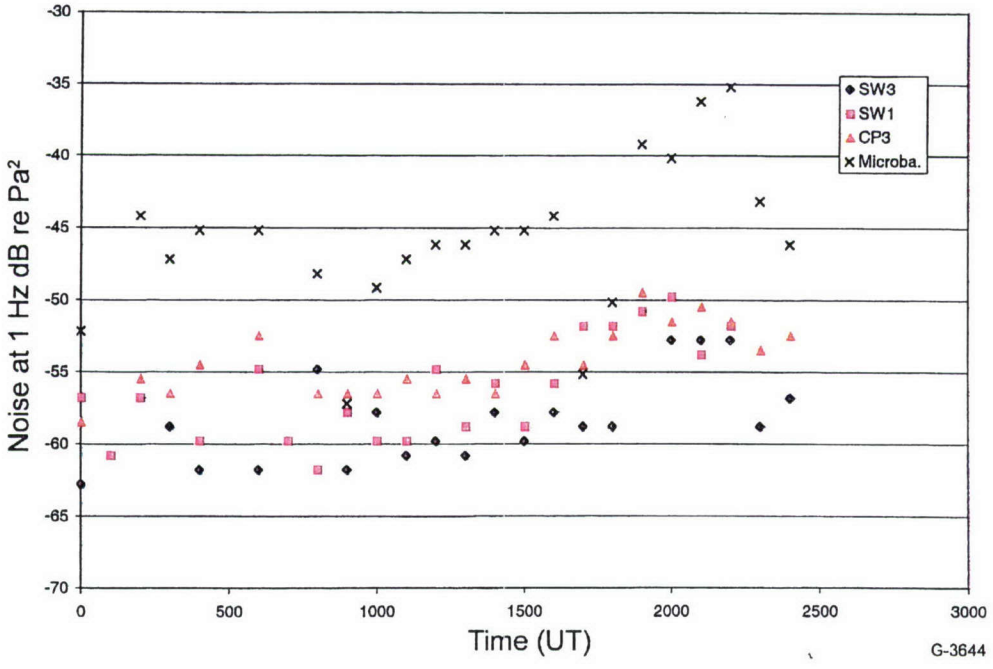


Figure 25. Averaged 1 Hz noise for E-W, 2 NS and microbarograph sensors for DOY 352.

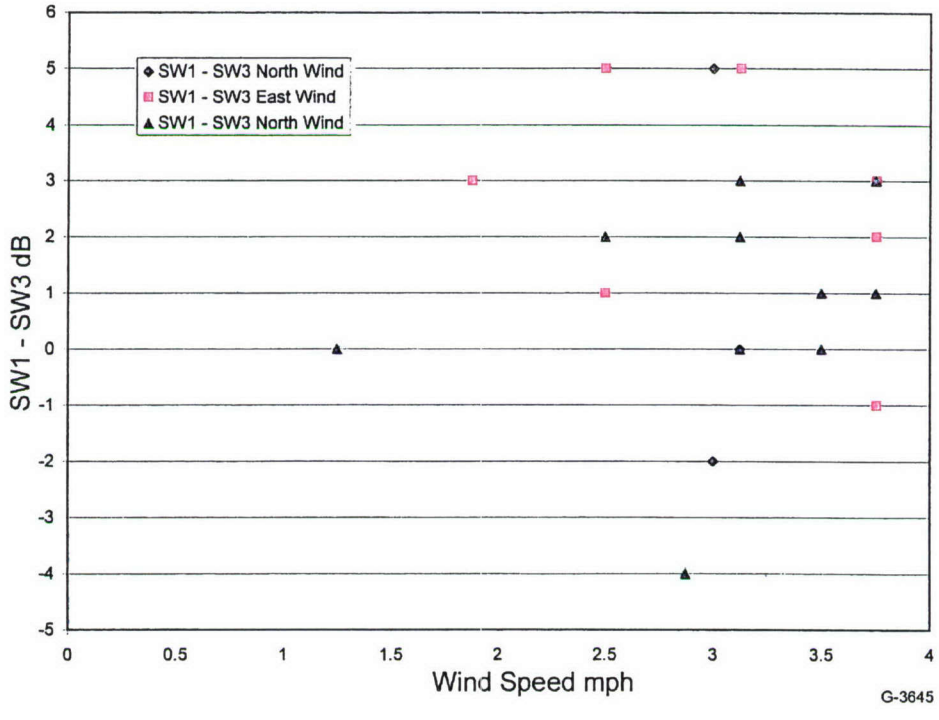


Figure 26. Difference in noise level average at 1 Hz for SW1-SW3.

Sensor CP3, which contains a braided shield, does not appear to have any noise advantage in this data, suggesting that electromagnetic noise is not an important factor at Pinon Flat or that the shielding employed is not effective.

### 2.7.3 Day 348 - A Higher Wind Example

During DOY 348, the wind speed never dropped below 12 mph, which provided a high wind test case. Figures 27 and 28 show the levels for SW3, SW1, CP3 and MB for portions of this day for which data were available as a function of time and estimated wind speed. Wind direction was uniformly from the West while this data was taken. The general trend observed at lower wind speeds that noise increases with wind speed continues at higher wind speeds, indicating that wind is probably the most important factor in piezocable noise.

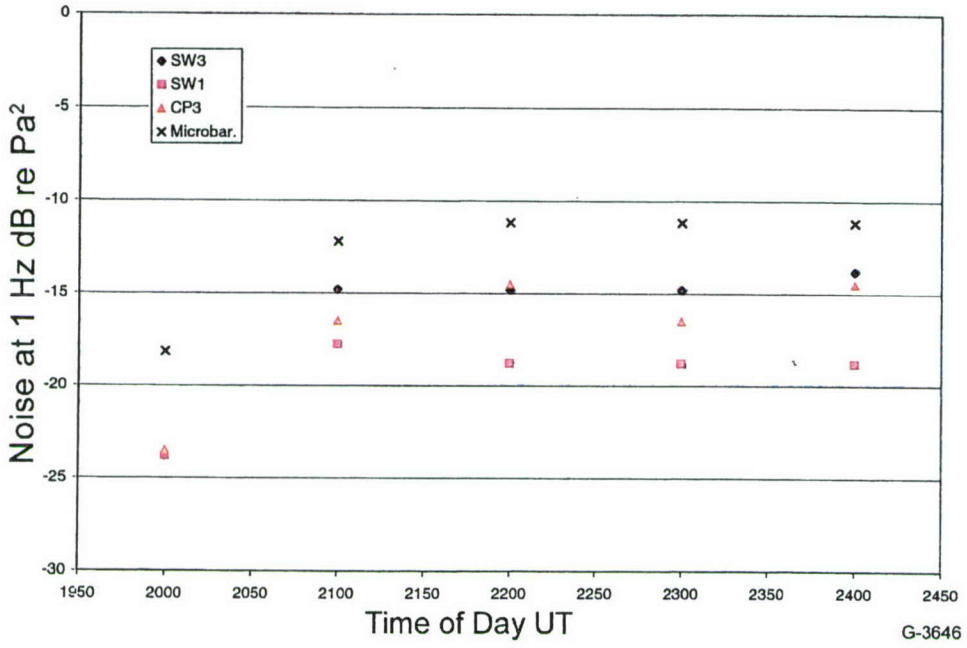


Figure 27. Averaged 1 Hz noise during DOY 348, a day with relatively high wind speeds.

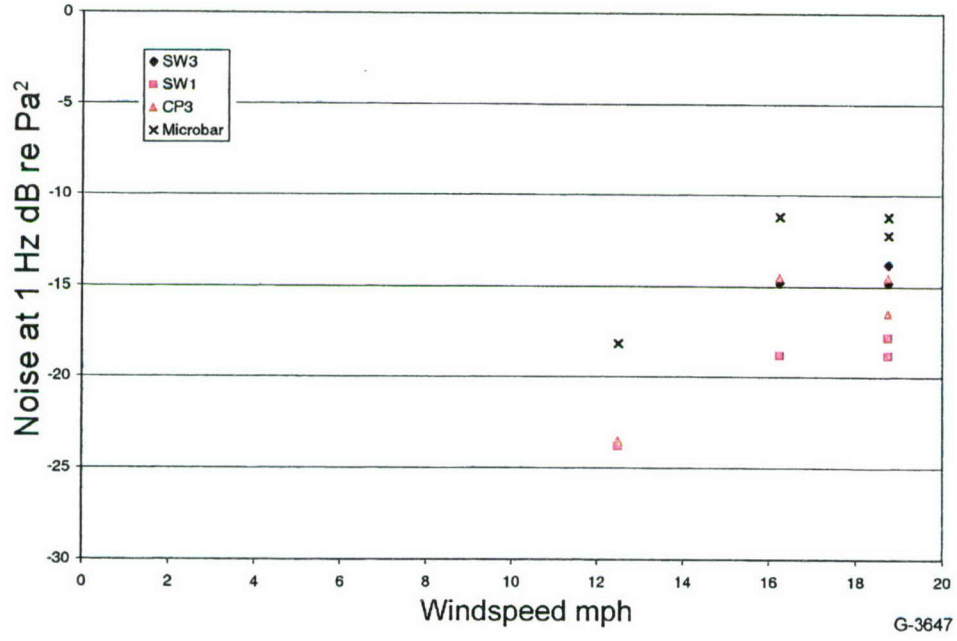


Figure 28. Averaged 1 Hz noise plotted vs wind speed.

At higher wind speeds, the microbarograph is consistently noisier by 5 to 15 dB than the piezocables. SW3 (parallel to wind direction) tends to be the noisiest piezocable, and SW1 (perpendicular to wind direction) tends to be the lowest. This suggests an interesting proposition, that the wind fields have less correlation perpendicular to their direction than parallel to it. Any testing of this hypothesis would require more data than is now available to us.

As it was for lower wind speeds, CP3 is consistent with other, non wire braid shielded sensors, suggesting again that electrical noise is not an important factor at Pinon Flat, though the shielding would be ineffective against magnetic disturbances at the low frequencies of interest for this program.

### 2.7.4 Two Interesting Signals

Figure 29 shows the period DOY 351 13:12:30 to 13:13:30, which includes a 20-second long signal containing energy around 5 Hz that appears on SW1, CP3, and SW3 with peak to peak amplitude on the order of 1 -2 mV on the piezocables but not on CP4, the second curve, or the microbarograph, the fifth curve. It begins almost exactly at 13:12:50 on the sensors in the North-South trench and it appears to begin about a second later on SW3 in the East-West trench. This would imply a 50 m/s travel velocity between sensor acoustic centers. It continues at about the same level until approximately 13:13:20 and remains visible in the time trace to 13:13:30 and appears to continue beyond the end of this time trace at a level on the order of a tenth of a millivolt.

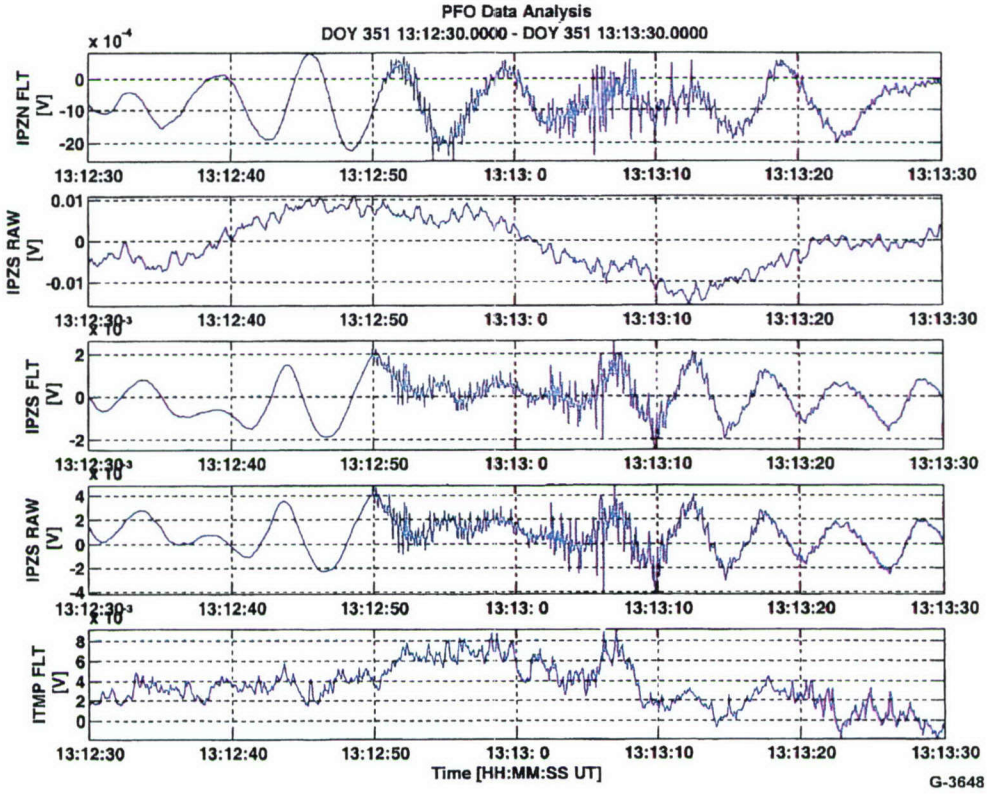


Figure 29. Time signals for DOY 351 showing curves for SW3, CP4, SW1, CP3 and the microbarograph.

An expanded view from 13:13:5 to 13:13:10 in Figure 30 shows that this signal is also present in CP4 at about the same amplitude as the other piezocables, and in the microbarograph as well. However, given the higher sensitivity of the latter for acoustic waves, this indicates that the microbarograph sensitivity to this signal is about a tenth of its acoustic sensitivity. This is similar to the characteristic response shown in Figure 15 for the DOY 356 earthquake.

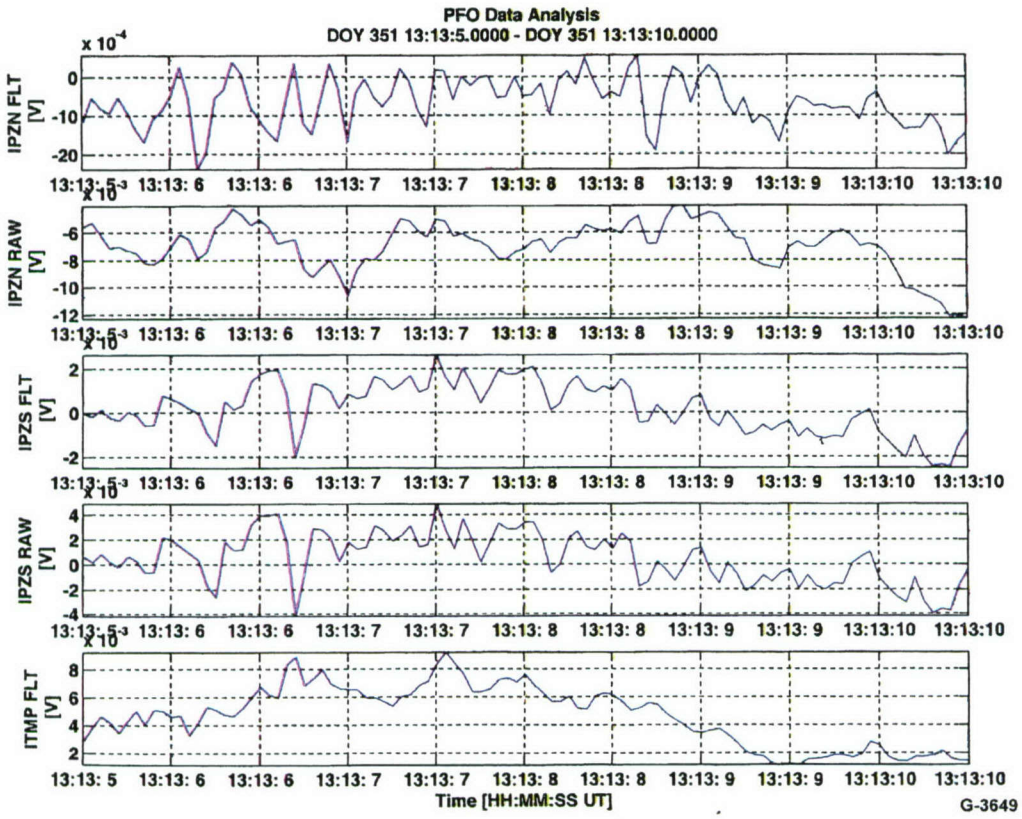


Figure 30. Signals with substantial 5 Hz components shown from top to bottom for SW3, CP4, SW1, CP3 and the microbarograph.

A similar signal from earlier in DOY 351 shown in Figure 31 appears on all four piezocables but is not apparent on the microbarograph. Given their unusual properties, including the insensitivity of the microbarograph to them, and their occurrence 5 days before the Central California earthquake, it is reasonable to suggest that these signals may be seismic rather than infrasonic, and may have been precursors to that earthquake. It would be good to compare these signals with seismic signals recorded at Pinon Flat when the data becomes available.

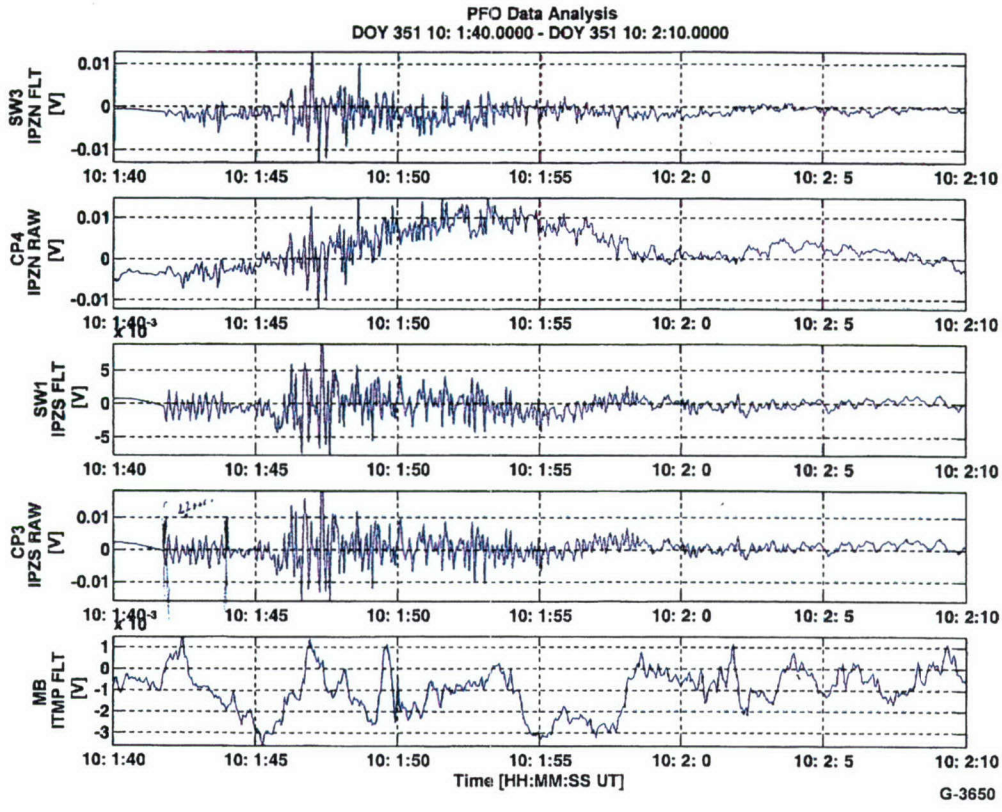


Figure 31. Time signals from earlier in DOY 351 that may have been there before the DOY 356 earthquake.

### 2.7.5 Hawaii Data

The next three plots (Figures 32 through 34) show data collected in December 2003. All three cables ...1, ...2, ...3, and the microphone ...4, show similar time traces. Figure 35 shows spectra of Figure 36. In January the similarity between the time traces is much less and the signal output from the calibration inserts - Figures 38 and 41, seem to indicate a partially shorted out condition for the ...3 sensor. No contract time is left to further analyze this data. See Figures 37 through 41 for additional data.

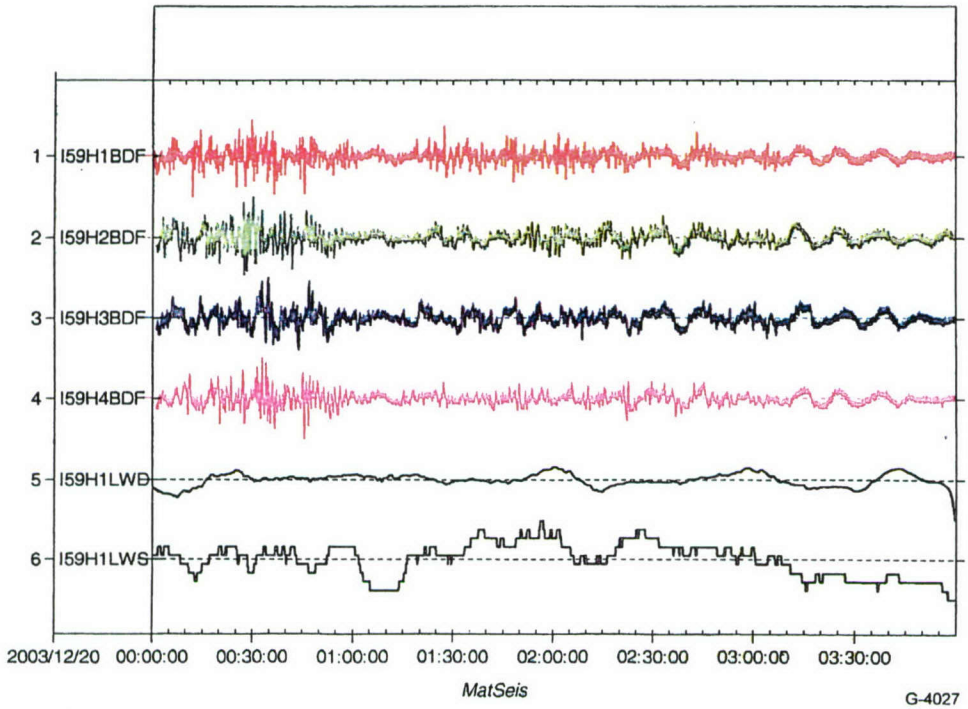


Figure 32. Time data from the north, west and south piezocable sensors and a microphone deployed at 159 US plus wind direction and speed measured nearby from 12:00 to 4:00 a.m. local time DOY 354.

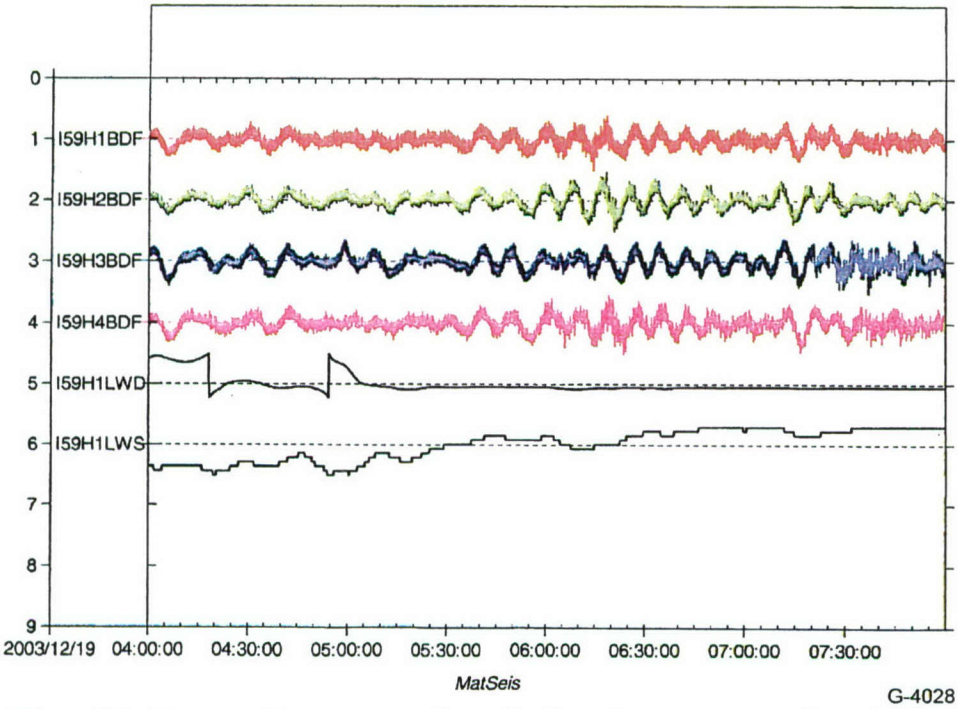


Figure 33. Time data from north, west, south, and microphone sensors plus wind direction and speed from 4:00 a.m. to 8:00 a.m. local time DOY 354.

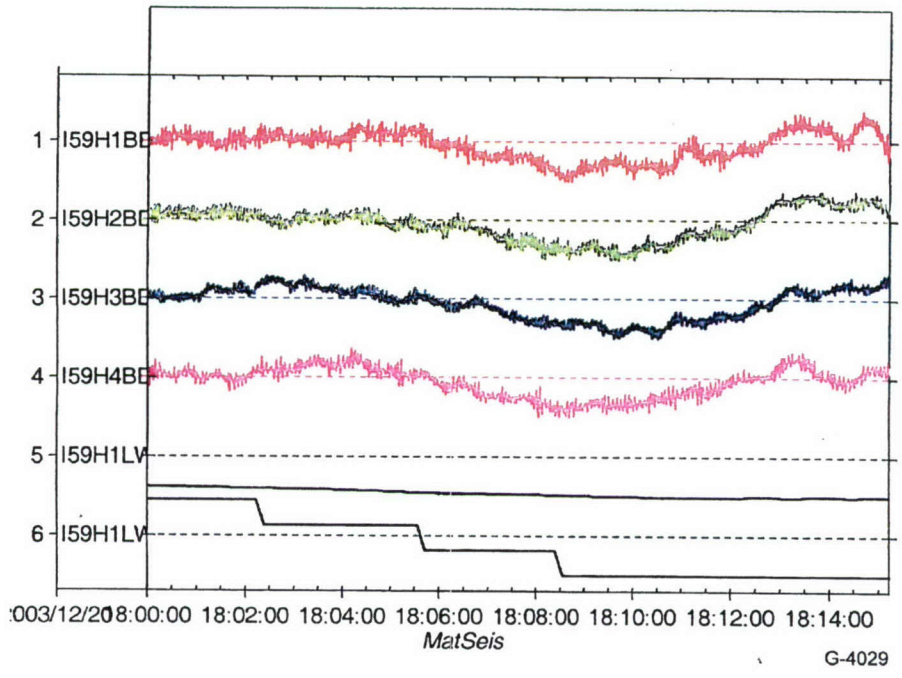


Figure 34. Time data from the north, west, south, and microphone sensors plus wind direction and speed from 6:00 p.m. to 6:15 p.m. local time DOY 354, showing expanded time and similar responses.

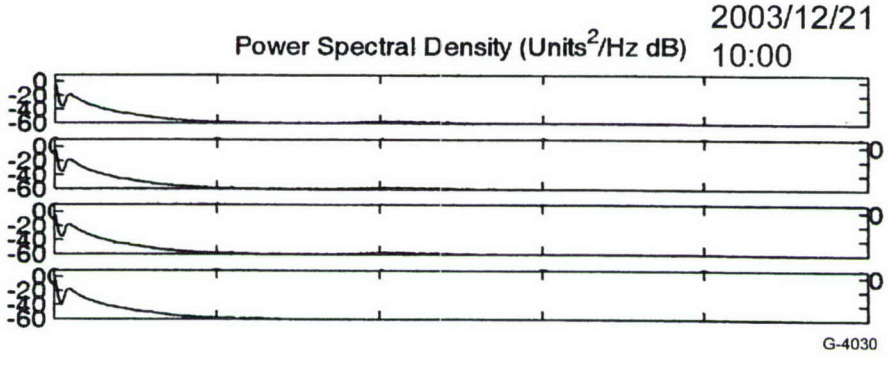


Figure 35. Spectral data for the four sensors shown in Figure 36 for the period 10:00 through 10:14 a.m. local time DOY 355. Note the low frequency peak corresponding to microbaroms at about 0.20 Hz, likely from breaking waves.

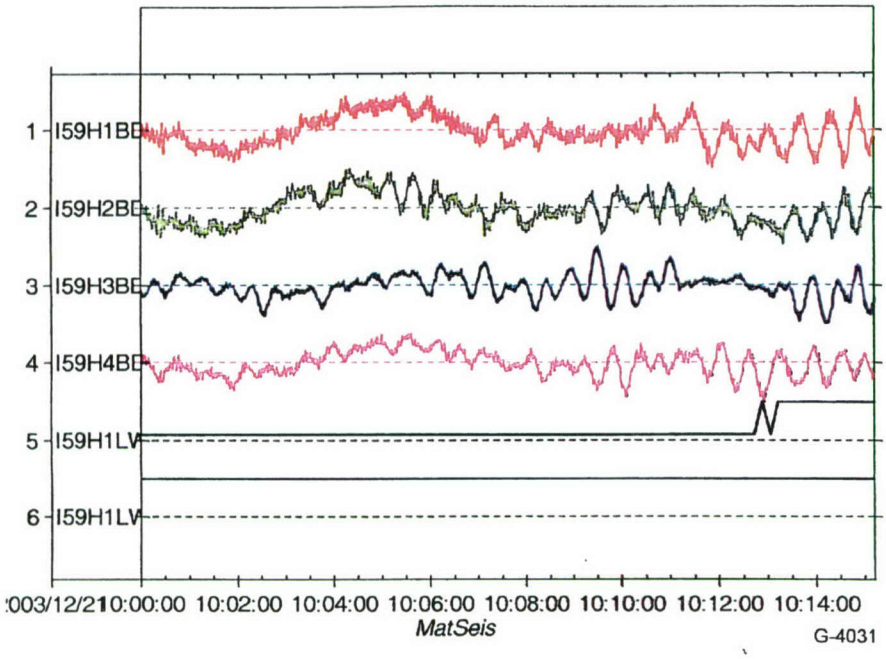


Figure 36. Time data from the north, west, south, and microphone sensors plus wind direction and speed from 10:00 a.m. to 10:15 a.m. local time DOY 355, showing expanded time and similar responses.

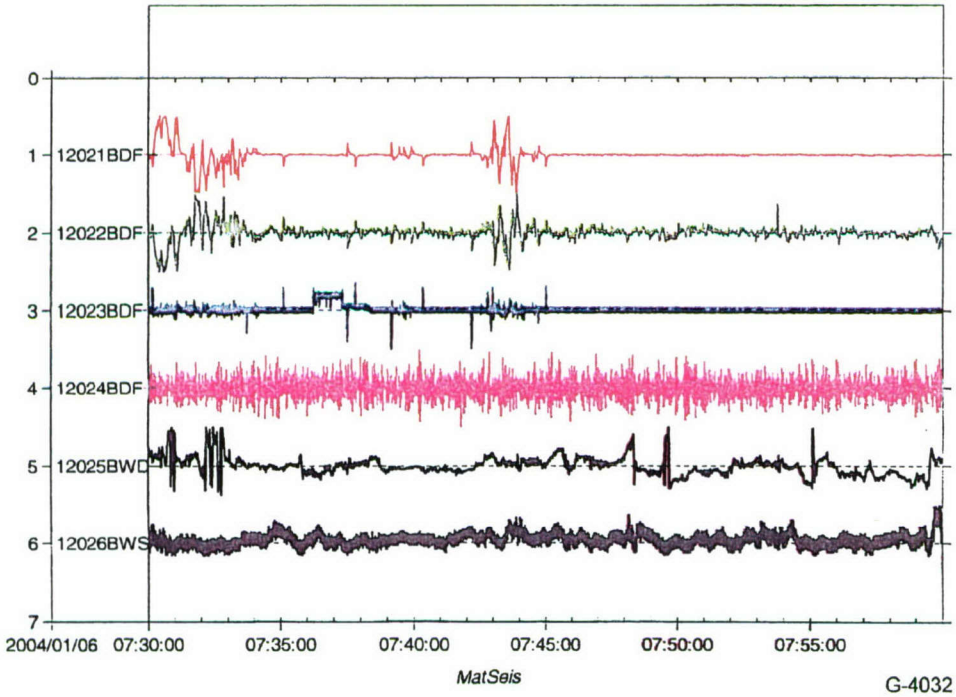


Figure 37. Time data from the north, west, south, and microphone sensors plus wind direction and speed from 7:30 to 8:00 a.m. local time DOY 006, showing expanded time and similar responses.

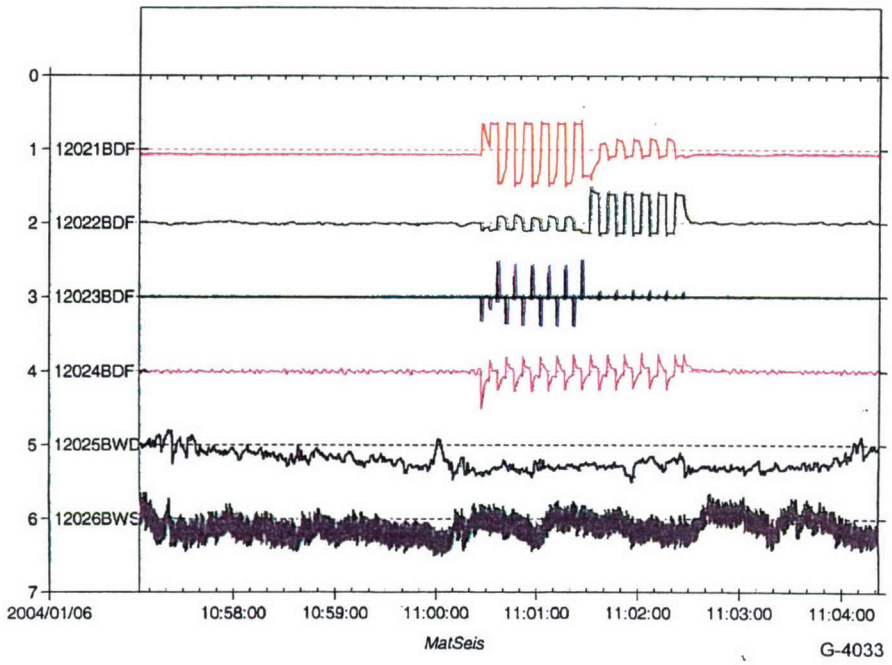


Figure 38. Expanded time trace showing the insert calibration signals from the piezocable amplifiers in the top three curves, DOY 006. Note probable effect of supply voltage drop on microphone output shown on fourth curve.

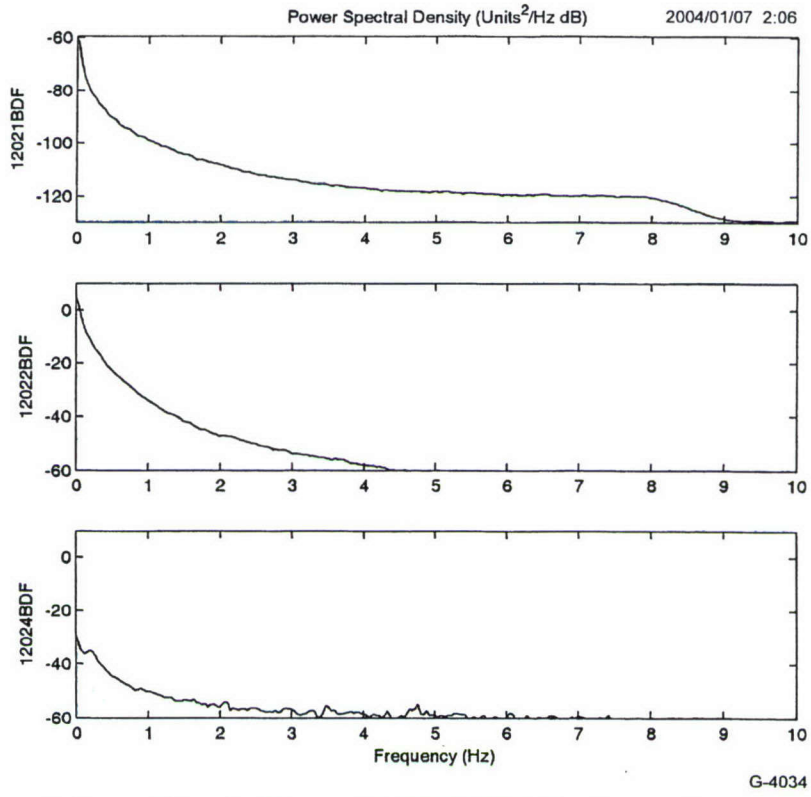


Figure 39. Spectral plots of data in Figure 40, DOY 007, for the north, west and south sensors. Extraneous noise is getting into the west and south sensors somehow.

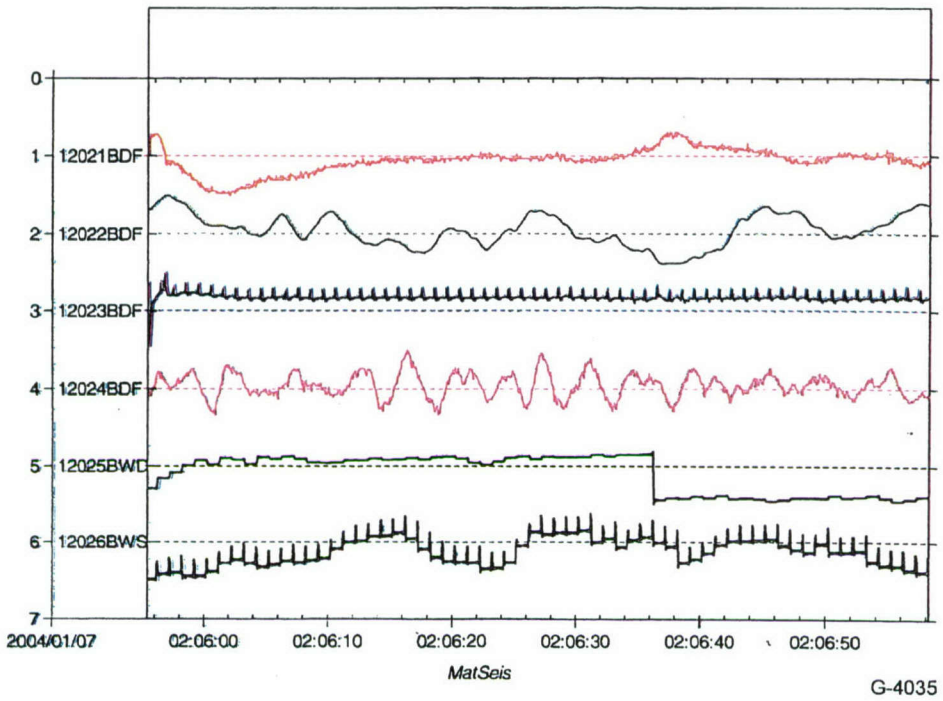


Figure 40. Expanded time trace of data taken on DOY 007 from 2:05:56 to 2:06:58 a.m. local time. Note south signal picking up timing pulses shown on wind speed curve.

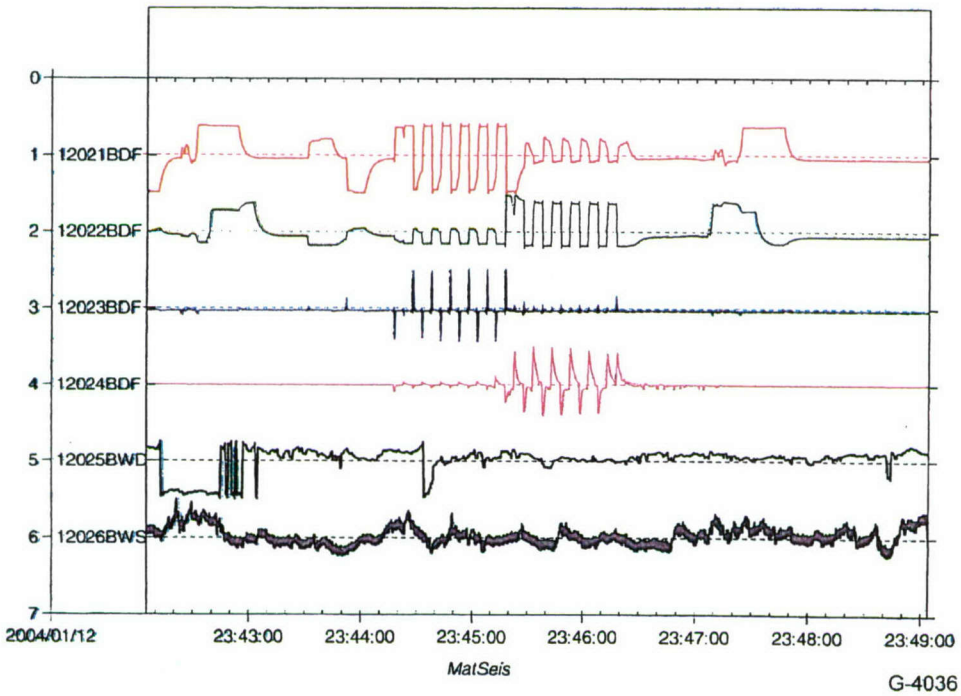


Figure 41. Expanded time trace showing the insert calibration signals from the piezocable amplifiers in the top three curves, DOY 012. Note probable effect of supply voltage drop on microphone output shown on fourth curve.

## 2.8 Summary

Our work over the last several years has demonstrated that piezocable sensors are an inexpensive, easy to install means to measure infrasound. They can be deployed over a large aperture with flexible geometries and provide direct pressure to electronic transduction, at the speed of light. Electronically-formed arrays can provide directivity, signal enhancement, aliasing mitigation, and small scale noise rejection. On-site or remote reconfigurations can be easily achieved to adjust to changing site conditions. Furthermore, arrays can be made robust, requiring little site preparation and support. Consequently they can be rapidly and easily deployed and removed.

Piezocable sensor/amplifier systems have demonstrated performance that meets CTBT noise specifications. A variety of acoustic events and microbaroms have been detected with anticipated sensitivity and are well correlated with data taken by permanent arrays at Pinon Flat. Spatial averaging via cable length selection has been demonstrated as has a means to infer signal incidence direction, and to reduce wind generated noise.

Currently there is a nine piezocable array prototype installed at Pinon Flat that can be operated continuously. A second prototype three sensor array was installed in Hawaii in late December. These arrays can provide valuable data and hands-on experience with independent verification of operation via comparisons with permanent arrays at the same sites.

Measurements made following the Central California earthquake indicate that the shallow buried cables can also sense seismic activity, possibly leading to a low-cost combined acoustic/seismic sensor for CTBT applications.

# 3. Conclusions

1. Burying of piezocables is essential to control wind generated noise. Deeper installation may reduce noise slightly. (Although data are not shown here, shallow burying 1 to 2 ft deep in the OFIS gravel trench at Pinon Flat proved less effective than deeper burying 6 to 12 ft in our two trenches.)

2. Use of thermal foam jacketing to control thermal noise does not appear to provide an obvious benefit, not does it appear to reduce sensitivity to acoustic or seismic signals.

3. Overall, buried 100 m piezocables have lower self noise than the UCSD microbarograph equipped with noise cancellation hoses. Piezocables appear to have a 10 to 15 dB advantage in light winds, and a 5 to 10 dB advantage in winds up to about 20 mph. In very lowest wind conditions, the microbarograph is sometimes slightly quieter than the piezocable.

4. Piezocable signal reception sensitivities in the field are consistent with theoretical and measured calibrations in the vicinity of 1 Hz, where most acoustic signal events occur.

5. Using the nominal sensitivities of piezocables, levels of observed microbarom energy are an order of magnitude larger than that measured by the microbarograph. This may be due either to a falloff in sensitivity of the microbarograph at lower frequencies, or to some kind of sensitivity enhancement due to ground motion at low frequencies.

6. Noise levels observed on CP3, the externally braid shielded sensor, are generally comparable to those on the unshielded cables, suggesting that electrical noise is not a significant factor, at least at Pinon Flat, or that this type of shielding is not effective against the noise as defined and quantified in this review.

**DEPARTMENT OF DEFENSE**

DEFENSE TECHNICAL
INFORMATION CENTER
8725 JOHN J. KINGMAN ROAD,
SUITE 0944
FT. BELVOIR, VA 22060-6201
2 CYS ATTN: DTIC/OCA

DEFENSE THREAT REDUCTION
AGENCY
8725 JOHN J. KINGMAN ROAD
STOP 6201
FT. BELVOIR, VA 22060-6201
2 CYS ATTN: NTD/D. BARBER

**DEPARTMENT OF DEFENSE CONTRACTORS**

ITT INDUSTRIES
ITT SYSTEMS CORPORATION
1680 TEXAS STREET, SE
KIRTLAND AFB, NM 87117-5669
2 CYS ATTN: DTRIAC
ATTN: DARE

PHYSICAL SCIENCES INC.
20 NEW ENGLAND BUSINESS
CENTER
ANDOVER, MA 01810
ATTN: F. KERN